Search for Bioactive Natural Products Targeting Hedgehog Signaling Pathway

A dissertation submitted in partial fulfillment of the requirements for the degree of Doctor of Philosophy

2011

Yusnita Rifai

Laboratory of Natural Products Chemistry

Graduate School of Pharmaceutical Sciences

Chiba University

Declaration

I certify that this thesis does not contain material which has been accepted for the award of any degree or diploma; and to the best of my knowledge and belief it does not contain any material previously published or written by another person except where due reference is made in the the text of this thesis.

Yusnita Rifai

September, 2011

Contents

Acknowledgements

I owe an enormous debt to my Ph.D supervisor, Professor Masami ISHIBASHI, head of Natural Product Chemistry Laboratory, Graduate School of Pharmaceutical Sciences, Chiba University, Japan. I sincerely express my respect and thankfulness for his time, scientific guidance and endless encouragement throughout my research program.

I also express my respect and gratitude to Assoc. Prof. Dr. Midori A. ARAI, for her scientific feedback, valuable discussion and help in many ways which enable me to accomplish this work on time.

Surely, this thesis would not have been possible without constant assistances and constructive suggestions from both Professor Masami ISHIBASHI and Assoc. Prof. Dr. Midori A. ARAI. I would like to say that I feel lucky of being a student of them because I have learned not only knowledge but also gained a lot of enthusiasm for scientific research.

I also would like to thank Professor Tsutomu ISHIKAWA for introducing me to Professor Masami ISHIBASHI in the very early of my Ph.D candidature in Chiba University.

I am grateful to Assist. Prof. Kazufumi TOUME for various help during the research work. I am indebted to the staff of Faculty of Pharmaceutical Science and the International Student Center for their cooperation and administrative help.

It was my greatest pleasure of working with past and present members of Natural Products Chemistry Laboratory, who gave me both help and friendship. Thanks to Dr Takashi Ohtsuki, a former Asistant Professor, Dr. F. Ahmed, Mr. Tateno, Mr. Fujimatsu, and Mr. Minakawa. I also would like to thank all fellow graduate students in the laboratory, whom I spent many joyous times with over the years and helped to make this experience memorable for me.

Moreover, none of this would have been possible without the love and patience of my husband Dr. Tasrief Surungan and my beloved son and daughter, Muhammad Attar Musharih and Sharien Musharih. My heartfelt gratitude to them for their endless support. Heartfelt thanks also go to my parents, H. Abd Rifai Tamri and Hj. Marhiah So'na including all my sisters and brother for continuously wishing me with good health and happiness.

I acknowledge the support of Hasanuddin University which has provided me a study leave for the completion of my degree since April 2008.

Lastly but much more important, I thank the Ministry of Education, Science and Culture, Japan for the financial support given through Monbukagakusho that enabled me to pursue Ph.D program in Chiba University.

Above all, praise be to the Almighty Allah, the Lord of the universe, to Whom all that exist will ever return.

Preface

Hedgehog (Hh) signaling regulates numerous events in embryonic development and adult tissue maintenance. Damage to essential core components of the Hh pathway often results in congenital birth defects whereas an aberrant activated Hh pathway leads to cancer.[1] The signaling begins with the binding of Hh protein ligand to its membrane receptor PTCH, which represses the activity of Smoothened (Smo). Smo in turn promotes the expression of GLI (Glioma-associated oncogene) family of transcription factors, leading to tumor development (Figure 1).[2]

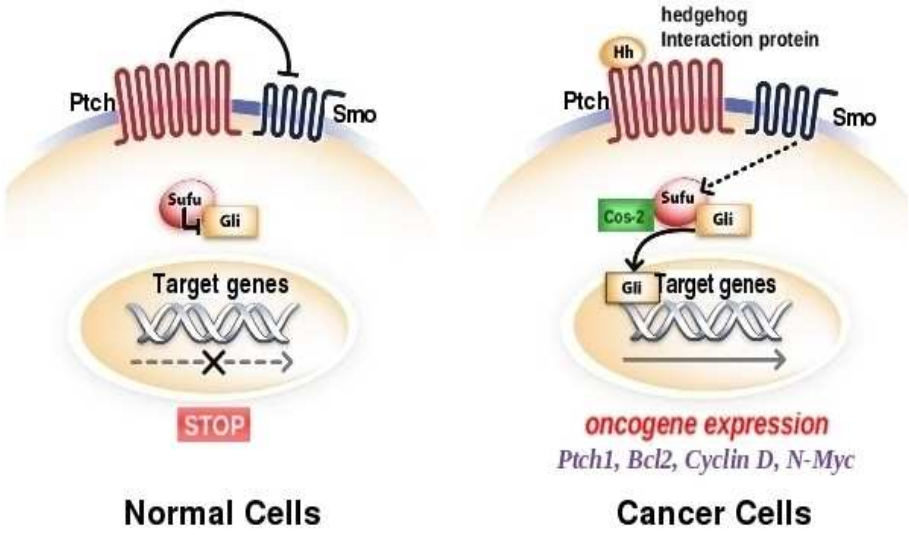

Figure 1: Hh Signaling pathway (A) In the absence of Hh signaling, Smo localizes mainly to the cell membrane (B) In the presence of Hh, repression of Smo by Ptch is relieved. Smo repression will activate GLI proteins, leading to oncogene expression.

GLIs, which are zinc-finger transcription factors, are known to regulate several genes, including cell cycle control-related genes and Hh/GLI signaling.[3] There are 3 GLI genes in vertebrate cells; GLI1, GLI2 and GLI3. Evidence suggests that GLI1 and

GLI2 represent the main activators of Hh target genes, while GLI3 acts mainly as repressor.[4]

Unlike GLI2 and GLI3, which are considered latent transcriptional regulators, GLI1 represents a direct transcriptional Hh-target gene. This transcriptional effector is closely associated with tumor formation by direct association with a specific binding site (5'-GACCACCCA-3') in the promoter region of the target genes.[5]

The Hh/GLI signaling is constitutively activated in several types of human tumors such as basal cell carcinoma and medullablastoma due to mutations in Ptch or Smo. This mutation will activate GLI1-mediated transcription hence cause tumor formation and progression.[6] In Hh signaling, GLI1 is considered to participate in the final step of the activation.

The regulation of GLI1 in mediating oncogenic Hh signaling is poorly known. Some reports describe that activated mutations of Smo induce the nuclear translocation of transcriptional GLI factors.[7,8] The use of small molecule inhibitors of Smo showed potentially limited efficacy. These inhibitors only treat tumors where pathway activation has occurred upstream or at the level of Smo, yet cancer with other downstream components is unresponsive to Smo inhibitors.[9]

Although there is a well-documented role for the Hedghog signaling pathway in cancer, there are relatively few synthetics and naturally occurring Hh signaling antagonists available that target GLI1 (GANTs).[10] Other sites that were mainly targeted are Smo protein (cyclopamine,[11,12] SANTs,[13] and CUR61414[14]) and Hh ligand (robotnikinin[15]) (Figure 2). Three synthetics are now entering clinical phase-1 studies (HhAntag691, GDC-0449, and BMS-833923).[16]

Given the essential role of Hh signaling pathway in the development of cancer as well as the prominent role of natural products in drug discovery, there remains an urgent need to find more potent Hh signaling inhibitors from natural resources.

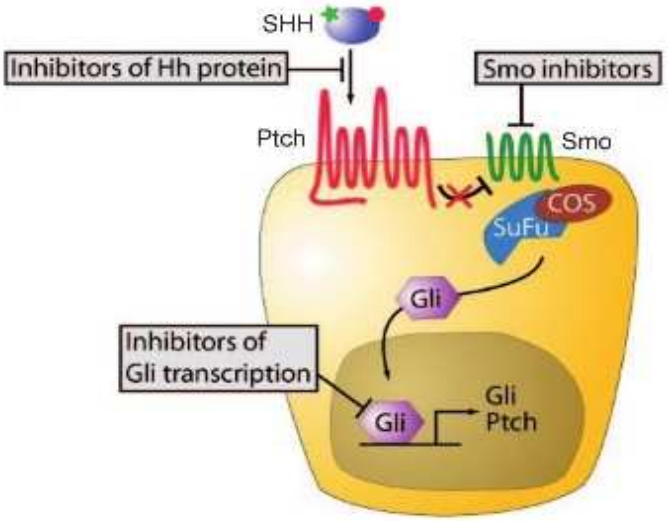

Figure 2: Components of the Hh signaling pathway and molecular sites targeted by Hh pathway inhibitors.

To identify naturally occuring inhibitors of the Hh/GLI signaling pathway, Professor Masami ISHIBASHI and his group reported the successful construction of a cell-based screening assay system[17] and have recently isolated several naturally occurring Hh/GLI inhibitors.[18–23] This thesis presented the search for small molecule inhibitors from natural resources interfering with GLI function.

To screen natural product libraries, a previous constructed cell screen of expressed exogenous GLI1 in HaCaT under tetracycline control (T-REx system) was used.[17] To identify the cell viability of compounds, a fluorometric microculture cytotoxicity (FMCA) method[24] was performed. A screening program has identified *Acacia pennata, Excoecaria agallocha, Vallaris glabra, Ocimum gratissimum* and *Piper chaba* as hit plants. These plants were further isolated, guided by Hh/GLI signaling inhibition. The inhibition of GLI-mediated transcriptional activity, cytotoxicity, and the effect of selected inhibitors on protein expression were further examined.

References

1. Ruiz, A. A.; Sanchez, P,; Dahmane, N. *Nat. Rev. Cancer* **2002**, *2*, 361-372.

2. Rubin, L. L.; de Sauvage, F. *J. Nat. Rev. Drug Disc.* **2006**, *5*, 1026-1033.

3. Eichberger, T.; Sander, V.; Schnidar, H., Regl, G.; Kasper, M,; Schmid, C.; Plamberger, S.; Kaser, A.; Aberger, F.; Frischauf, A. M. *Genomics* **2006**, *87*, 616-632.

4. Aza-Blanc, P.; Lin, H. Y.; Ruiz i Altaba, A.; Konberg, T. B. *Development* **2000**, *127*, 4293-4301.

5. Kinzler, K. W., Vogelstein, B. Mol. *Cell. Biol.* **1990**, *10*, 634-642.

6. Johnson, R. L.; Rothman, A. L.; Xie, J.; Goodrich, L. V.; Bare, J. W.; Bonifas, J. M.; Quinn, A. G.; Myers, R. M.; Cox, D. R.; Epsten Jr, E. H.; Scott, M. P. *Science* **1996**, *272*, 1668-1671.

7. Pasca di Magliano, M., Hebrok, M. *Nat. Rev. Cancer* **2003**, *3*, 903-911.

8. Jacob, L., Lum, L. *Science* **2007**, *318*, 66-68.

9. Taylor, M. D., Liu, L., Raffel, C., Hui, C. C., Mainprize, T. G., Zhang, X., Agatep, R., Chiappa, S., Gao, L., Lowrance, A., Hao, A., Goldstein, A. M., Stavrou, T., Scherer, S. W., Dura, W. T., Wainwright, B., Squire, J. A., Rutka, J. T., Hogg, D. *Nat. Genet.* **2002**, *31*, 306-310.

10. Lauth, M., Bergstrm, A., Shimokawa, T., Toftgrd, R. *Proc. Natl. Acad. Sci. U.S.A.* **2007**, *104*, 8455-8460.

11. Chen, J. K., Taipale, J., Cooper, M. K., Beachy, P. A. *Genes Dev.* **2002**, *16*, 2743-2748.

12. Incardona, J. P., Gaffield, W., Kapur, R. P., Roelink, H. *Development* **1998**, *125*, 3553-3556.

13. Chen, J. K., Taipale, J., Young, K. E., Maiti, T., Beachy, P. A. *Proc. Natl. Acad. Sci. U.S.A.* **2002**, *99*, 14071-14076.

14. Williams, J. A., Guicherit, O. M., Zaharian, B. I., Xu, Y., Chai, L., Wichterle, H., Kon, C., Gatchalian, C., Porter, J. A., Rubin, L. L., Wang, F. Y. *Proc. Natl. Acad. Sci. U.S.A.* **2003**, *100*, 4616-4621.

15. Stanton, B. Z., Peng, L. F., Maloof, N., Nakai, K., Wang, X., Duffner, J. L., Taveras, K. M., Hyman, J., Lee, S. W., Koehler, A. N., Chen, J. K., Fox, J. L., Mandinova, A., Schreiber, S. L. *Nat. Chem. Biol.* **2009**, *5*, 154-156.

16. Peukert, S.; Miler-Moslin, K. *ChemMedChem* **2010**, *5*, 500-512.

17. Hosoya, T.; Arai, M. A.; Koyano, T.; Kowithayakorn, T.; Ishibashi, M. *Chembiochem*, **2008**, *9*, 1082-1092.

18. Arai M, A.; Tateno, C.; Koyano, T.; Kowithayakorn, T.; Ishibashi, M. *Bioorg. Med. Chem.* **2008**, *16*, 9420-9424.

19. Rifai, Y.; Arai, M. A.; Koyano, T.; Kowithayakorn, T.; Ishibashi, M. *J. Nat. Prod.* **2010**, *73*, 995-997.

20. Rifai, Y.; Arai, M. A.; Sadhu, S. K.; Ahmed, F.; Ishibashi, M. *Bioorg. Med. Chem. Lett.* **2011**, *21*, 718-722.

21. Shintani, A.; Toume, K.; Rifai, Y.; Arai, M. A.; Ishibashi, M. *J. Nat. Prod.* **2010**, *73*, 1711-1713.

22. Arai, M. A.; Tateno, C.; Koyano, T.; Kowithayakorn, T.; Kawabe, S.; Ishibashi, M. *Org. Biomol. Chem.* **2011**, *9*, 1133-1139.

23. Rifai, Y.; Arai, M. A.; Koyano, T.; Kowithayakorn, T.; Ishibashi, M. *J. Nat. Med.* **2011**, *65*, 629-632.

24. Larsson, R., Kristensen, J., Sandberg, C., Nygren, P. *Int. J. Cancer* **1992**, *50*, 177.

Chapter 1

Assay Protocol

1.1 GLI Transcriptional Activity

Firefly luciferase, a 61 kDa monomeric protein, functions as a genetic reporter. The luciferase system is considered as a sensitive reporter assay for gene expression.

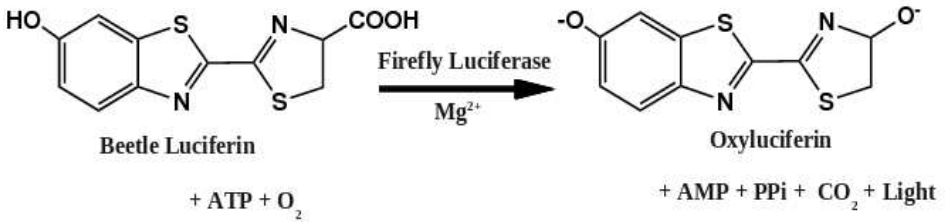

Figure 1.1: Luminescence reactions catalyzed by firefly

Principally, luminescence is achieved through oxidation of beetle luciferin in a reaction that requires ATP, Mg^{2+} and O_2 (Figure 1.1). The oxidation occurs through a luciferyl-AMP intermediate that results in a $flash$ of light. The $flash$ rapidly decays after the substrate and enzyme are mixed.

GLI transcriptional activity was calculated from the ratio of the reporter luciferase activity of sample-treated cells/non-treated cells ;

$$\text{GLI transcriptional activity (\%)} = \frac{\text{the reporter luciferase activity of sample-treated cells}}{\text{the reporter luciferase activity of control (DMSO)}} \times 100$$

1.2 Cell Viability

Cell viability of sample was measured by Fluorometric Microculture Cytotoxicity Assay[1] (FMCA) method using Fluorescein Diacetate (FDA) as a dye. FDA is a nonfluorescent compound which is converted to fluorescence intensity. The assay is based on hydrolysis of the probe, FDA by esterases in cells with intact plasma membranes (Figure 1.2). The conversion is directly proportional to the number of viable cells which is calculated as follows:

$$\text{Cell Viability (\%)} = \frac{\text{fluorescence of sample-treated cells}}{\text{fluorescence of control (DMSO)}} \times 100$$

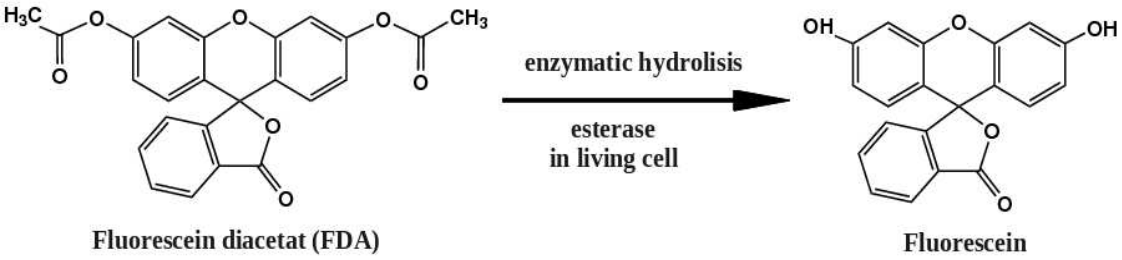

Figure 1.2: The conversion by viable cells of fluorescein diacetate to fluorescent fluorescein

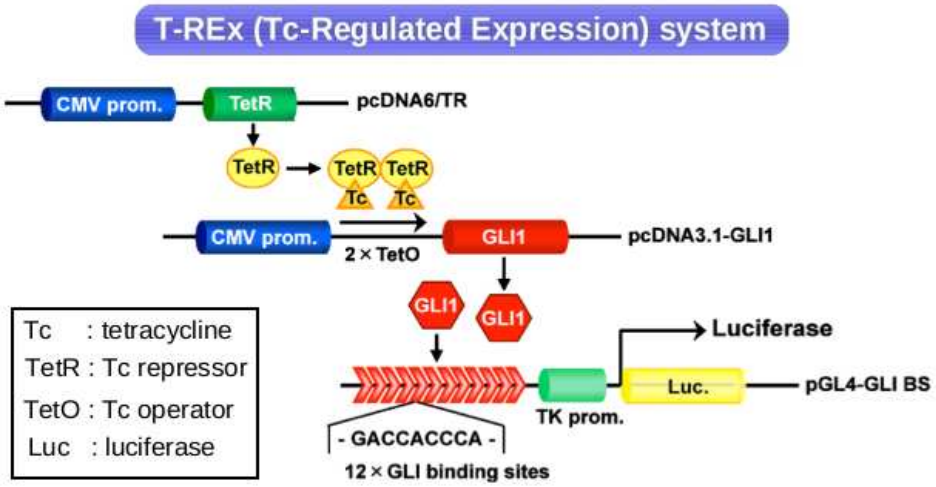

Figure 1.3: Constructed Screening System

1.3 Compound Screen

HaCaT cells were stably co-transfected with plasmid pcDNA3.1-GLI1, which produced exogenous GLI1 proteins, together with the reporter plasmid pcDNA3.1-GLI-luc, which produced luciferase by GLI1-mediated transactivation and pcDNA6/TR. In this compound screening, tetracycline, which introduces exogenous GLI1 overexpression, was removed when compounds were added to HaCaT-GLI1-Luc cells (Tet-On system) (Figure 1.3).

Cells (HaCaT-GLI1-Luc) were seeded in a 96-well white plate at 2 x 10^4 per well. After 12 h incubation at 37 ^{0}C, tetracycline (Tc) 1 μg/mL was added and cells were incubated for another 12 h. Compounds were added at various concentrations and subsequently, luciferase activity was measured on a microplate luminometer (Thermo) using the Bright-GloTM Luciferase Assay System (Promega) according to the manufacturer's protocol. Simultaneously, the cell viability of the compound-treated cells was measured by FMCA using a fluorescence plate reader (Thermo)

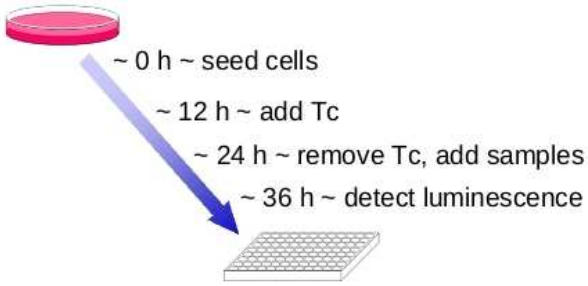

Figure 1.4: Hh/GLI-Signaling Inhibitory assay

(Figure 1.4).

As depicted in Figure 1.5, light orange bar represents luciferase activity and dark orange represents the viability of sample. If the percentage of luciferase activity is low but the percentage of cell viability high, compound is considered to positively inhibit Hh/GLI signaling.

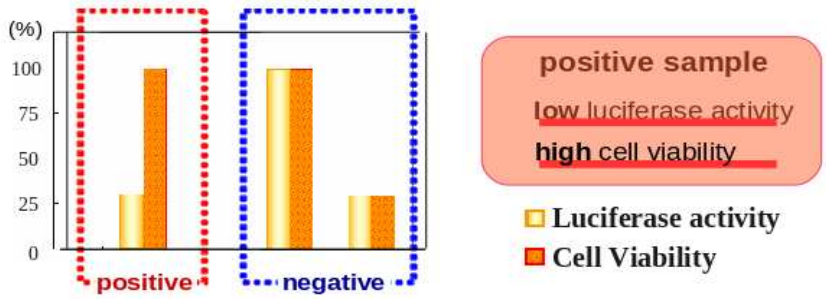

Figure 1.5: Hh/GLI-Signaling Inhibitory activity of compounds

1.4 Cytotoxicity Test

PANC1, C3H10T1/2 (RIKEN BRC) or DU145 (Cell Resource Center for Biomedical Research Institute of Development, Aging and Cancer, Tohoku University) were

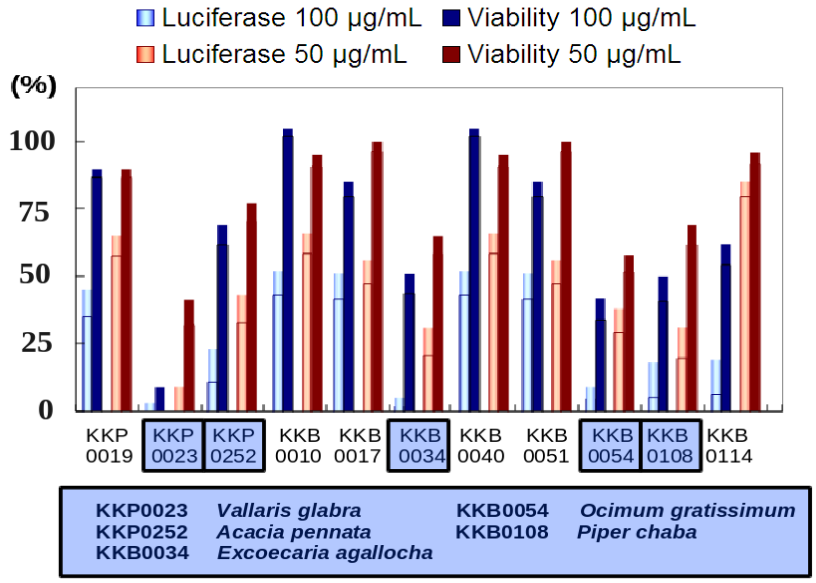

Figure 1.6: Hh/GLI-Signaling inhibition of some medicinal plant extracts collected from Thailand (KKP0019: *Nauclea orientalis*) and Bangladesh (KKB0010: *Sida rhombifolia*, KKB0017: *Ficus racemosus*, KKB0040: *Rhizophora mucronata*, KKB0051: *Alombus meruensis*, KKB0114: *Boerhavia diffusa*).

seeded in black 96-well plates at 1 x 10^4 cells per well. After incubation at 37 ^{0}C for 24 h, medium was replaced by compounds at different concentrations. Cell proliferation was determined by FMCA, and IC_{50} values were determined. Assays were performed in triplicate.

1.5 Screening of Plant Extract Library

Medicinal plants, collected from Thailand (KKP) and Bangladesh (KKB), were screened for Hh/GLI-Signaling Inhibition. About 73 Bangladesh plants (KKB001-KKB0057 and KKB101-KKB117) were screened and the inhibitory activity charts were attached at Appendix I. Activity of some selected extracts is shown in Figure 1.6.

Activity of KKP0019, KKP0023, and KKP0252, showed in Figure 1.6, were screened by Mr. Chikashi Tateno in 2009.

References

1. Larsson, R., Kristensen, J., Sandberg, C., Nygren, *P. Int. J. Cancer*, **1992**, *50*, 177.

2. Hosoya, T.; Arai, M. A.; Koyano, T.; Kowithayakorn, T.; Ishibashi, M.*Chembiochem*, **2008**, *9*, 1082-1092.

3. Arai M, A.; Tateno, C.; Koyano, T.; Kowithayakorn, T.; Ishibashi, M. *Bioorg. Med. Chem.* **2008**, *16*, 9420-9424.

Chapter 2

Separation of *Acacia pennata*

The leaves of *Acacia pennata* (Figure 2.1), locally in Thailand known as *cha-om*, are used in indigenous systems of medicine. Although several compounds were reported from *Acacia pennata* including alkaloids, saponins, polysachharides, terpenoids, condensed tannins and flavonoids[1], relatively little is known about the pharmacological effect of this plant.

2.1 Extraction and Isolation

Leaves (10.0 g) of *Acacia pennata* were extracted with MeOH. The MeOH extract was partitioned with hexane (200 mL x 3), EtOAc (200 mL x 3), and BuOH (200 mLx 3). The EtOAc-soluble fraction (1.9 g) was subjected to silica gel column chromatography (40 x 260 mm), and eluted successively with a gradient mixture of hexane-EtOAc-MeOH (10:2:1 to 2:2:1) to yield 6 fractions (2A to 2G). Fraction 2D (390.3 mg) was underwent ODS flash column chromatography (12 x 245 mm) to give fractions 3A-3J. Active fraction 3E (131.2 mg) was further separated by PSQ-100B silica gel column chromatography (30.3 mg), followed by passage over Sephadex LH-20 (10 x 150 mm), using methanol 100%, to afford compounds **1** (13.8

Figure 2.1: *Acacia pennata*

mg), **2** (3.0 mg), and **3** (3.7 mg). Fraction 1F (161 mg), separated from the hexane extract (0.98 g), was chromatographed over 60 N silica gel (20 x 450 mm), using hexane-CHCl3-EtOAc (from 16:1:1 to 0:2:1), to yield compound **4** (8.1 mg) and compound **5** (2.0 mg).

2.2 Structure Elucidation

Bioassay-guided separation of *Acacia pennata* (Figure 2.2) led to the isolation of 5 known compounds from hexane and EtOAc extracts. Compounds **1-5** were identified by comparing their spectroscopic data to literature values (Figure 2.3).

Taepeenin D (1)[2]

^{1}H and ^{13}C NMR data, see Table 2-1, EIMS *m/z* $[M + Na]^{+}$ 407

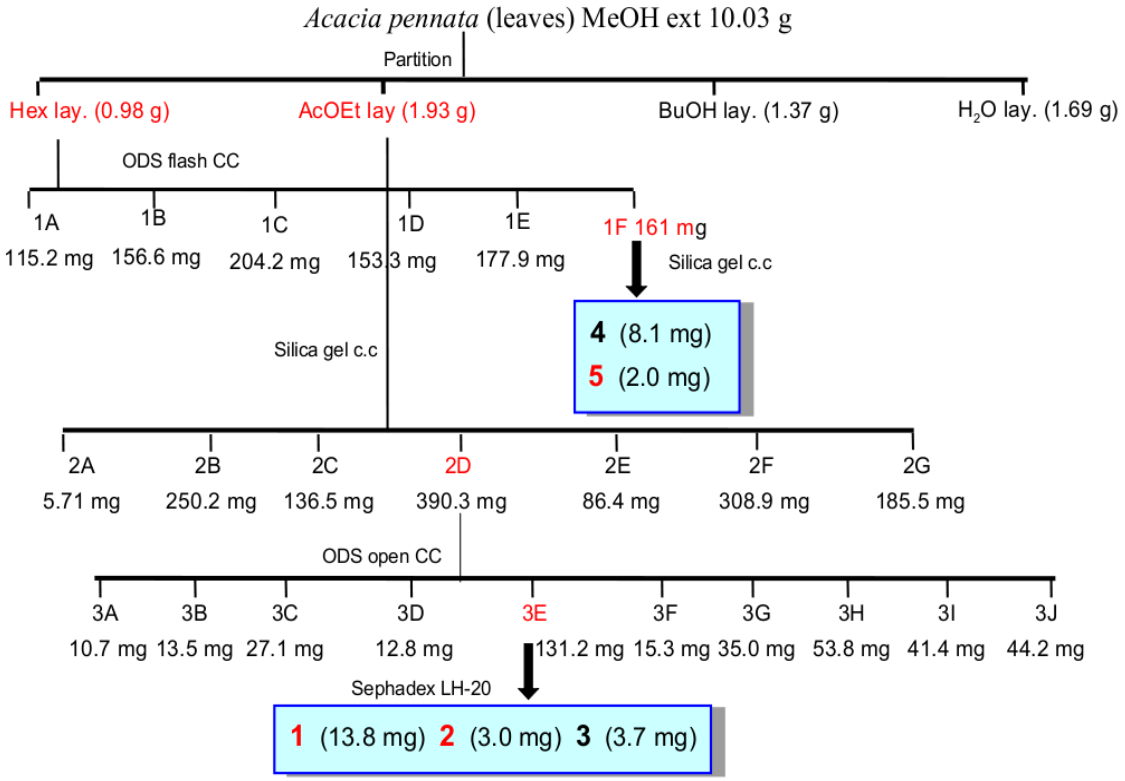

Figure 2.2: Isolation Scheme of *Acacia pennata*

Drimenin (2)[3]

^{1}H and ^{13}C NMR data, see Table 2-2, FAB MS *m/z* $[M + H]^+$ 207

Labdanolic acid (3)[4]

^{1}H and ^{13}C NMR data, see Table 2-3, EIMS *m/z* $[M + Na]^+$ 347, $[\alpha]_D^{23}$ -6.07 (*c* 0.35, MeOH)

8,15-labdanediol (4)[5]

^{1}H and ^{13}C NMR data, see Table 2-3, FAB MS *m/z* $[M + K]^+$ 349, $[\alpha]_D^{22}$ -5.37 (*c* 0.61, $CHCl_3$)

Quercetin-3-β-D-glucopyranosyl-4-O-β-D-glucopyranoside (5)[6]

^{1}H and ^{13}C NMR data, see Table 2-4, FAB MS m/z [M + Na]$^{+}$ 649

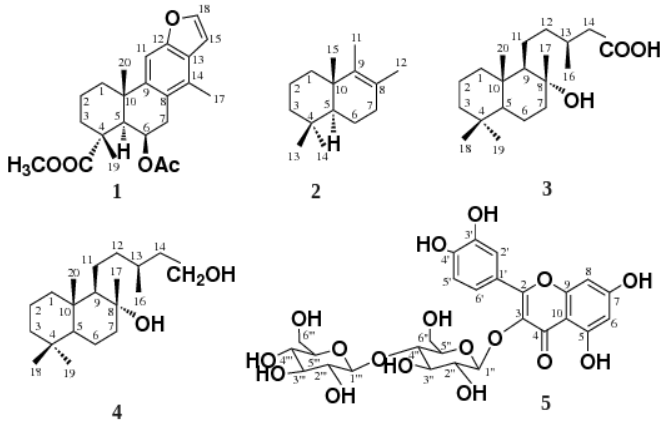

Figure 2.3: Structures of **1-5**

2.3 Activity Assay

The isolated compounds **1-5** were evaluated for their GLI-mediated transcriptional activity. Compounds **1**, **2**, and **5** inhibited Hh/GLI-mediated transcriptional activity with IC_{50} values of 1.6, 13.5, and 10.5 μM, respectively, whereas compounds **3** and **4** were inactive (Figure 2.4 A, Table 2-5).

As for cytotoxicity assays, a panel of cells was included with increased Hh signaling levels (PANC1 and DU145) and without reliance on Hh ligand for survival (C3H10T1/2). The results revealed that compounds **1**, **2**, and **5** were cytotoxic against PANC1 cells (IC_{50} values of 3.2, 15.1, and 26.6 μM, respectively) and DU145 cells (IC_{50} values of 3.4, 23.2, and 30.0 μM, respectively) but did not affect normal cell lines (Figure 2.4 B, Table 2-5).

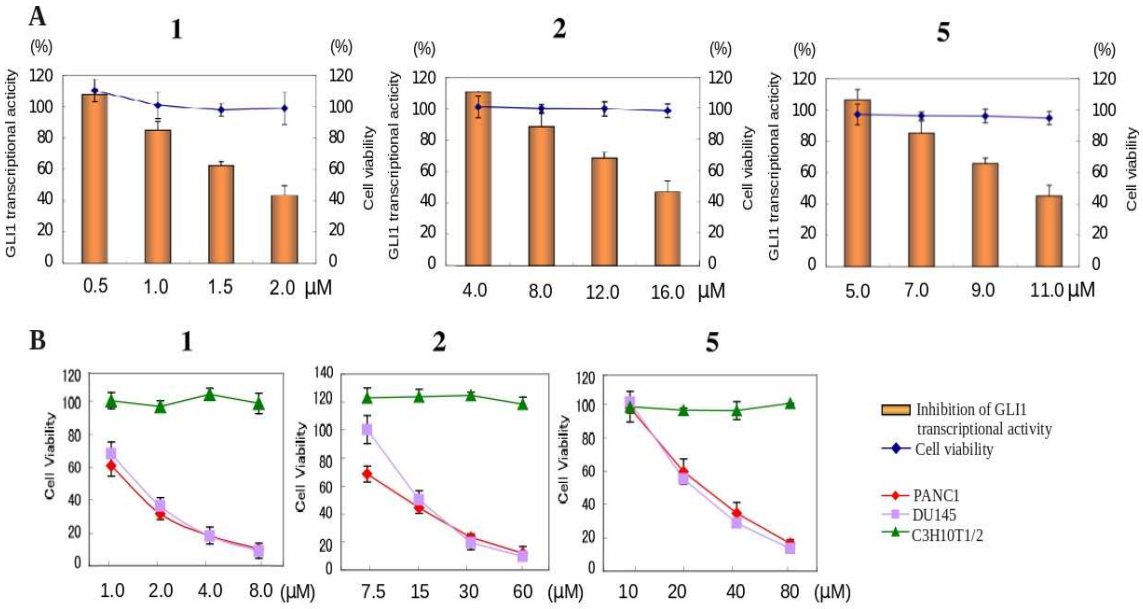

Figure 2.4: (A) Inhibition of GLI1-mediated transcriptional activity (solid columns) and cell viability (solid curves) of compounds **1**, **2**, and **5**. HaCaT-GLI1-Luc cells were seeded onto a 96-well plate (2 x 10^5 cells per well) then treated with compounds after 12 h tetracycline addition. Cell viability and luciferase activity were determined at the same time. The assays were performed at 0.05 % DMSO (n = 3). Error bars represent s.d. (B) Cytotoxicity of compounds **1**, **2**, and **5** against PANC1, DU145, and C3H10T1/2 cells. The assays were performed 0.05 % DMSO (n = 3). Error bars represent s.d.

GLI1 transcriptional factors are known to regulate expression of multiple targets including PTCH[7] and BCL-2.[8] Both proteins were over-expressed in HaCaT-GLI1-Luc cells and PANC1. Although compounds **1**, **2**, and **5** differently interfered with PTCH and BCL-2 proteins, western blot analysis confirmed that each compound reduced the expression of both proteins in a concentration-dependent fashion (Figure 2-5). It is also important to note that the GLI1 protein level in HaCaT cells decreased for compound **1** but not for compounds **2** and **5**. In this assay, tetracycline, which introduces exogenous GLI1 over-expression, was removed when compounds

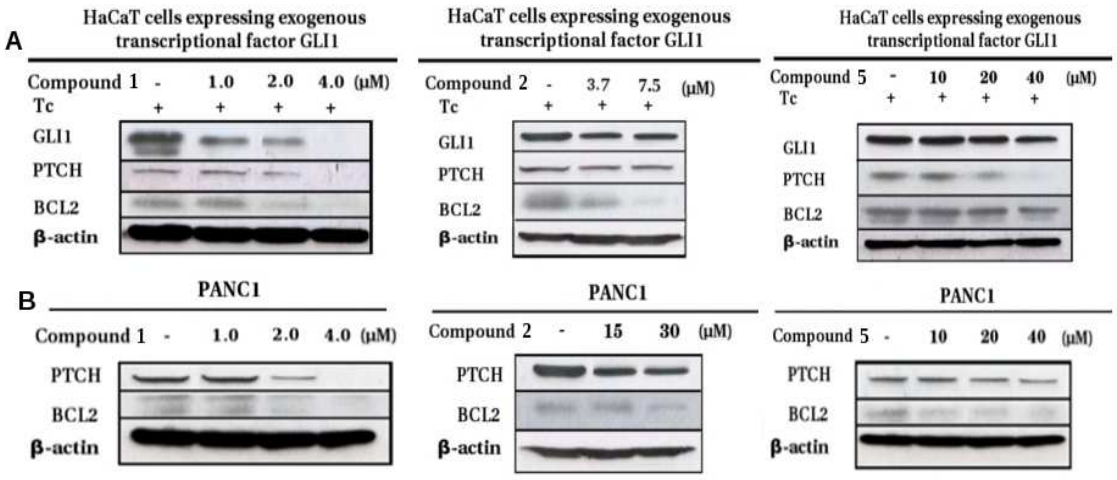

Figure 2.5: Inhibition of GLI-related protein (PTCH and BCL2) levels by compounds **1**, **2**, and **5**. (A) Treatment of **1**, **2**, and **5** on GLI1-overexpressing HaCaT cells. (B) Treatment of **1**, **2**, and **5** on PANC1 cells.

were added to HaCaT-GLI1-Luc cells. Therefore, compound **1** might accelerate GLI1 protein degradation in HaCaT-GLI1-Luc cells. These results thus indicated that different structures had different target molecules.

Furthermore, the inhibition of Ptch mRNA expression by taepeenin D (**1**) in PANC1 was examined using real time-PCR analysis. Cyclopamine, a steroidal alkaloid that inhibits the Hh response,[9] was included as a positive control. The antagonism of Smo was reported previously as a target of cyclopamine action.[10,11] As depicted in Figure 2.6, treatment of **1** at 2 and 4 μM reduced the mRNA expression of Ptch compared to a negative control. Similar trend of inhibition was apparent on the mRNA expression of cyclopamine-treated cancer cells. A report by Chatel *et al.* highlighted the fact that treatment of cyclopamine (10 μM) modulated Ptch expression in PANC1 due to the inhibition of Gli1 mRNA level,[12] thereby suggesting that taepeenin D (**1**) is also an effective inhibitor of the Hh signaling pathway.

In conclusion, three constituents of *Acacia pennata* leaves were found to inhibit Hh

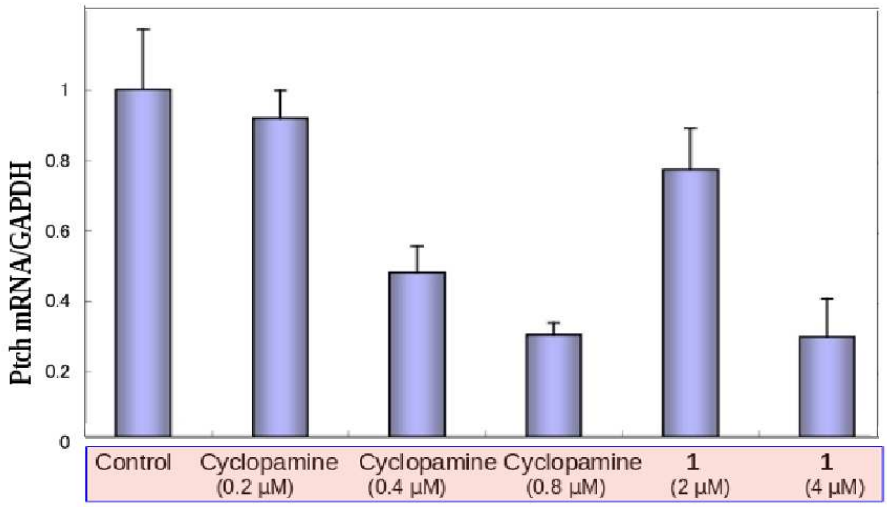

Figure 2.6: Inhibition of GLI1-mediated mRNA expression of Ptch by compound **1** in PANC1 cells. GAPDH was used as an internal control. The assays were performed at 0.05 % DMSO (n = 3). Error bars represent s.d.

signaling. This inhibition was caused by downregulated Ptch mRNA expression along with decreased protein level of PTCH and BCL-2 in HaCaT cells expressing exogenous GLI1 and PANC1 cells.

References

1. Seigler, D. S. *Biochemical Systematics and Ecology* **2003**, *31*, 845-873.

2. Cheenpracha, S.; Srisuwan, R.; Karalai, C.; Ponglimanont, C.; Chantrapromma, K.; Fun, H.; Anjum, S.; Atta-ur-Rahman. *Tetrahedron* **2005**, *61*, 8656-8662.

3. Iida, T.; Yoshii, E.; Takeshima, K.; Nakata, T.; Tani, Y.; Oishi, T. *Yakugaku Zasshi* **1980**, *100*, 915-919.

4. Bolster, M. G.; Jansen, B. J. M.: de Groot, A. *Tetrahedron* **2001**, *57*, 5657-

5662.

5. de Pascual, T. J.; Urones, J. G.; Marcos, I. S.; Nunez, L.; Basabe, P. *Phytochemistry* **1983**, *22*, 2805-2808.

6. Ohmoto, T.; Nikaido, T.; Nozaki, T.; Ikuse, M. *Yakugaku Zasshi* **1977**, *97*, 176-180.

7. Agren, M.; Kogerman, P.; Kleman, M. I.; Wessling, M.; Toftgrd, R. *Gene* **2004**, *330*, 101-114.

8. Lum, L.; Beachy, P. A. *Science* **2004**, *204*, 1755-1759.

9. Cooper, M. K.; Young, K. E.; Beachy, P. A. *Science* **1998**, *280*, 1603-1607.

10. Taipale, J.; Chen, J. K.; Cooper, M. K.; Wang, B.; Mann, R. K.; Milenkovic, L.; Scott, M. P.; Beachy, P. A. *Nature* **2000**, *406*, 1005-1009.

11. Chatel, G; Ganeff, C.; Boussif, N.; Delacroix, L.; Briquet, A.; Nolens, G.; Winkler, R. *Int. J. Cancer* **2007**, *121*, 2622-2627.

Table 2-1. NMR Spectroscopic data for compound **1** (in $CDCl_3$)

Position	δ_C	δ_H (*J* in Hz)
1	42.1	2.36 (1H, m)
2	18.9	1.51 (1H, s) 1.80 (1H, m)
3	38.4	1.68 (1H, m) 1.80 (1H, m) 1.65 (1H, m)
4	48.0	2.50 (1H, br, s)
5	46.0	
6	70.6	5.30 (1H, d, 5.5)
7	34.7	3.12 (1H, dd, 18 , 5.2,) 2.98 (1H, d, 18)
8	123.7	
9	145.5	
10	37.9	
11	104.94	7.38 (1H, br, s)
12	153.7	
13	125.6	
14	128.6	
15	104.97	6.73 (1H, dd, 2.4, 0.9)
16	144.5	7.54 (1H, d, 2.4)
17	16.0	2.33 (3H, s)
18	178.6	
19	18.0	1.45 (3H, s)
20	27.5	1.60 (3H, s)
$-OCH_3$	52.4	3.71 (3H, s)
-OAc	21.7 170.6	2.00 (3H, s)

Table 2-2. NMR Spectroscopic data for compound **2** (in $CDCl_3$)

Position	δ_C	δ_H (*J* in Hz)
1	37.4	1.30 (2H, br, s)
2	19.4	1.41 (1H, m) 1.05 (1H, m)
3	41.5	1.20 (2H, d, 9)
4	33.1	
5	50.1	2.13 (1H, m)
6	19.6	2.04 (2H, m)
7	32.8	1.98 (2H, m)
8	124.5	
9	135.3	
10	38.5	
11	19.6	1.62 (3H, s)
12	19.8	1.68 (3H, s)
13	33.1	0.84 (3H, s)
14	12.3	0.87 (3H, s)
15	21.1	0.94 (3H, s)

Table 2-3. NMR Spectroscopic data for compounds **3** and **4** (in $CDCl_3$)

	Compound **3**		Compound **4**	
Position	δ_C	δ_H (*J* in Hz)	δ_C	δ_H (*J* in Hz)
1	39.8	1.37 (2H, m)	39.8	1.37 (2H, m)
2	18.4	1.39 (2H, m)	18.4	1.39 (2H, m)
3	42.5	1.30 (2H, m)	42.5	1.30 (2H, m)
4	33.1		33.1	
5	59.8	1.43 (2H, br, s)	59.8	1.43 (2H, br, s)
6	20.5	1.52 (2H, m)	20.5	1.52 (2H, m)
7	40.6	1.58 (2H, m)	40.6	1.58 (2H, m)
8	79.5		79.5	
9	62.7	2.04 (2H, m)	62.7	2.24 (2H, m)
10	38.4		38.4	
11	23.8	1.21 (2H, d, 6.1)	23.8	1.21 (2H, d, 6.1)
12	43.6	1.17 (2H, d, 6.1)	43.6	1.17 (2H, d, 6.1)
13	31.3	1.66 (1H, br, s)	31.3	1.66 (1H, br, s)
14	41.6	1.84 (1H, q, 7)	41.6	1.84 (1H, q, 7)
15	177.5		60.6	3.57 (1H, d, 6)
16	19.4	0.92 (3H, d, 5.6)	19.0	0.92 (3H, d, 6)
17	23.1	0.98 (3H, s)	23.1	0.98 (3H, s)
18	33.8	0.94 (3H, s)	35.8	0.94 (3H, s)
19	21.5	0.94 (3H, s)	21.5	0.94 (3H, s)
20	14.3	0.96 (3H, s)	14.2	0.96 (3H, s)

Table 2-4. NMR Spectroscopic data for compound **5** (in CD_3OD)

Position	δ_C	δ_H (*J* in Hz)	Position	δ_C	δ_H (*J* in Hz)
2	158.8		1''	105.3	5.15 (1H, d, 8)
3	135.6		2''	73.2	3.80 (1H, dd, 8, 9)
4	179.6		3''	75.1	3.55 (1H, d, 9)
5	163.2		4''	75.7	3.46 (1H, m)
6	99.9	6.21 (1H, d, 2)	5''	70.0	3.82 (1H, d, 8)
7	166.0		6''	61.9	3.56 (1H, 12, 2)
8	94.9	6.40 (1H, d, 2)			3.54 (1H, 12, 5)
9	158.5		1'''	105.4	5.25 (1H, d, 7)
10	105.4		2'''	77.2	3.47 (1H, dd, 7, 8)
1'	122.9		3'''	78.1	3.42 (1H, d, 7)
2'	117.8	7.64 (1H, d, 8.5)	4'''	78.4	3.33 (1H, m)
3'	146.1		5'''	71.2	3.88 (1H, ddd, 2, 10, 14)
4'	149.9		6'''	62.5	3.69 (1H, 14, 2)
5'	116.0	6.87 (1H, d, 8.5)			3.59 (1H, dd, 14, 4)
6'	123.2	7.59 (1H, dd, 2, 8.5)			

Table 2-5. IC_{50} Values of GLI-mediated Transcriptional Inhibition and Cytotoxicity against Cancer Cells (PANC1, DU145) and C3H10T1/2 Cell.

Compound	GLI transcriptional inhibition (IC_{50}, μM)	Cytotoxicity (IC_{50}, μM)		
		PANC1	DU145	C3H10T1/2
1	1.6	3.2	0.8	>100
2	13.5	15.1	22.0	>100
3	160.0	180.0	166.8	-
4	200.3	201.2	214.6	-
5	10.5	26.6	30.0	>100

Chapter 3

Separation of *Excoecaria agallocha*

Excoecaria agallocha Linn. (Euphorbiaceae) (Figure 3.1) is a mangrove tree that is widely distributed throughout the forests and swamps of the Sundarbans, in coastal areas of Bangladesh and in wetland along the coastline of China.[1] This plant, known locally as *Gewa*, has been traditionally used to treat skin irritation and potentially shows anti-tumor-promoting[2] and anti-HIV activities.[3] Previous phytochemical studies on *Excoecaria agallocha* revealed the presence of diterpenoids,[2,3] triterpenoids,[1] and flavonoids.[4]

3.1 Extraction and Isolation

The MeOH extract (20.5 g) was subjected to Diaon HP-20 column chromatography (50 x 250 mm) using mixtures of MeOH/acetone to yield MeOH-soluble fractions. This MeOH-soluble part (4.1 g) was partitioned with H_2O (200 mL) between hexane (200 mL x 3), and the aqueous phase was further extracted with EtOAc (200 mL x 3) and BuOH (200 mL x 3) to afford hexane extract (537.2 mg), EtOAc extract

Figure 3.1: *Excoecaria agallocha*

(2.62 g), BuOH extract (645.0 mg) and H_2O extract (252.5 g).

BuOH extract (645.0 mg) was chromatographed on a silica gel 60 N column (20 x 350 mm) using the increasing polarity of the MeOH : H_2O solvent system to afford fractions 3A-3F. Compounds **6** (15 mg), **11** (2.7 mg) and **12** (7.4 mg) were isolated from fraction 3D (69.2 mg), 3E (82.7 mg), and 3F (185.5 mg) respectively after silica gel 60 N column chromatography (16 x 400 mm) using $CHCl_3$: MeOH as the solvent system.

The EtOAc-soluble fraction (2.62 g) was subjected to ODS flash column chromatography (30 x 280 mm), and eluted successively with a gradient mixture of MeOH: H_2O (20 : 80 to 0 : 100) to yield 9 fractions (2A to 2I). Fraction 2C (430.6 mg) was subjected to Sephadex LH-20 column chromatography using MeOH as the eluent to obtain compound **8** (19.3 mg). Another active fraction from the EtOAc extract (fraction 2D, 234.4 mg) was underwent silica gel 60N column chromatography (25

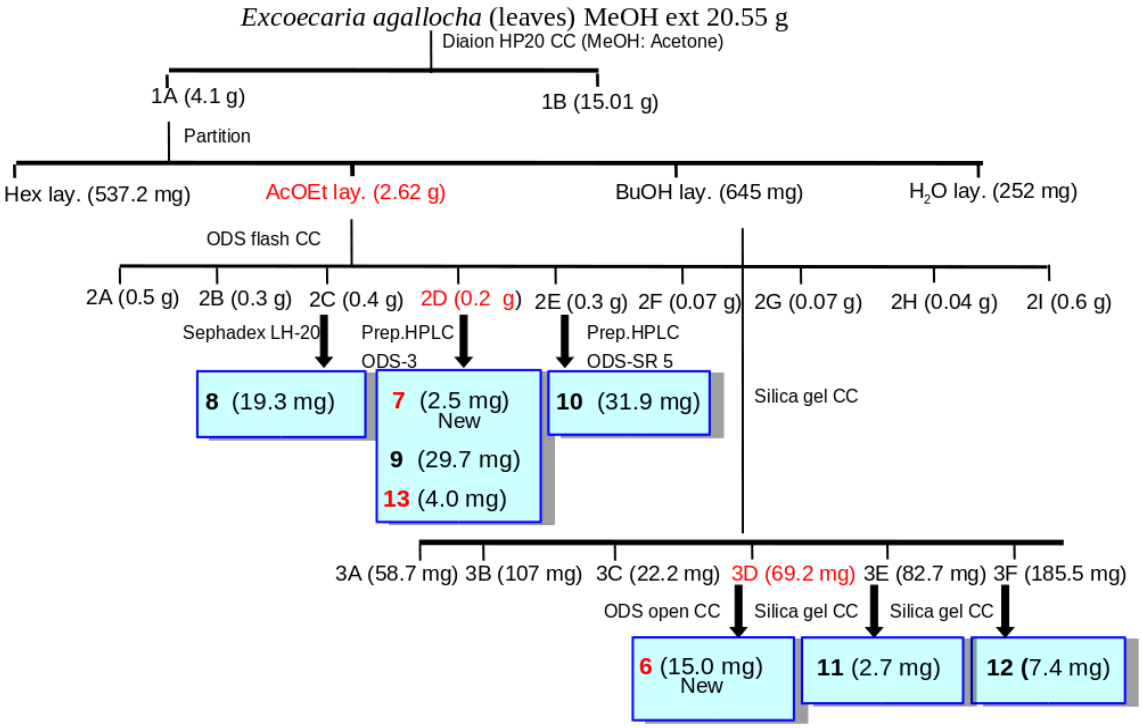

Figure 3.2: Isolation Scheme of *Excoecaria agallocha*

x 580 mm) and was eluted with increasing MeOH (30-100 %) in H_2O to give 11 fractions (4A-4K). Fractions 4F and 4K were determined as compounds **9** (29.7 mg) and **13** (4.0 mg) respectively. From 4J (11.7 mg), compound **7** (2.5 mg) were obtained after preparative HPLC (inertsil ODS-3, 10 x 250 mm; MeOH : H_2O (6 : 4); flow rate 1.5 mL min-1; RI and UV detection at 254 nm). Furthermore, fraction 2 E (312.1 mg) of the EtOAc extract was underwent preparative HPLC (inertsil ODS-5, 6.0 x 250 mm; MeOH : H_2O (7 : 3); flow rate 2.0 mL min^{-1}; RI and UV detection at 254 nm) to afford compound **10** (31.9 mg).

3.2 Structure Elucidation

Separation of *Excoecaria agallocha* guided by Hedgehog/GLI signaling inhibition led to the isolation of 2 new compounds (**6** and **7**) along with 6 known flavonoid

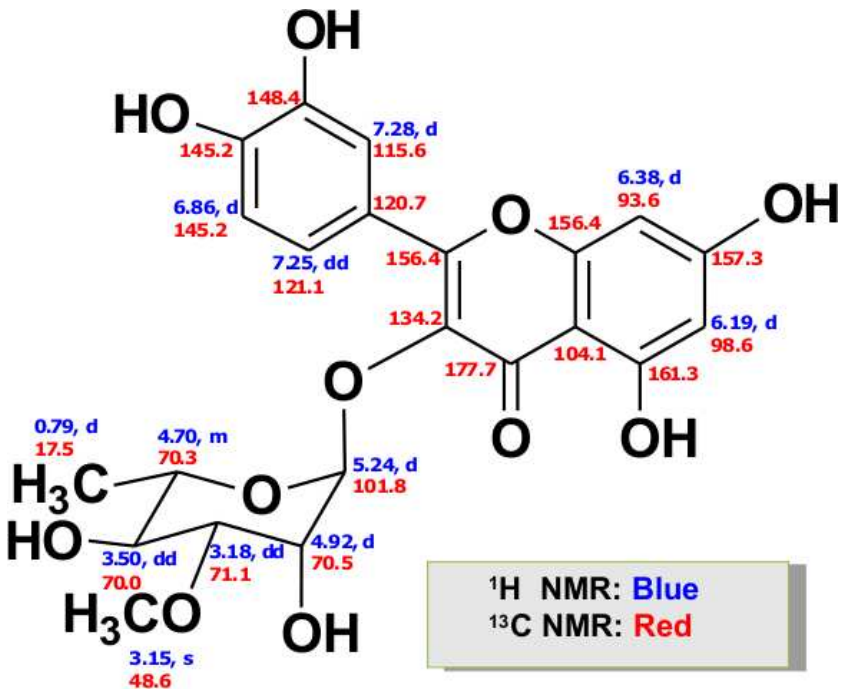

Figure 3.3: Structure of Compound **6**

glycosides (**8**-**13**) (Figure 3.2).

3.2.1 New Compounds

Compound **6** (Figure 3.3) was obtained as a yellow powder and had a molecular weight at m/z 485.1162 ([M+Na]$^+$, -2.1 mmu), corresponding to the molecular formula of $C_{22}H_{22}O_{11}$ in the HR-FABMS. The IR absorption bands suggested the presence of hydroxyl (3317 cm-^{1}) (br) and carbonyl (1680 cm-^{1}) groups. The UV absorption maxima were at UV (MeOH) λ max 261 nm (log ϵ 3.8) and 355 nm (log ϵ 3.0). Acid hydrolysis of compound **6** gave quercetin and acofriose (3-*O*-methyl rhamnose). Acofriose was determined as having an L-form by comparison of its specific rotation $[\alpha]_D^{22}$ +35 (c 0.1, MeOH) with those reported in the literature $[\alpha]_D^{22}$ +39.[5] The carbon signals at δ_C 177.7 (C-4), 148.4 (C-3') and 145.2 (C-4') were in

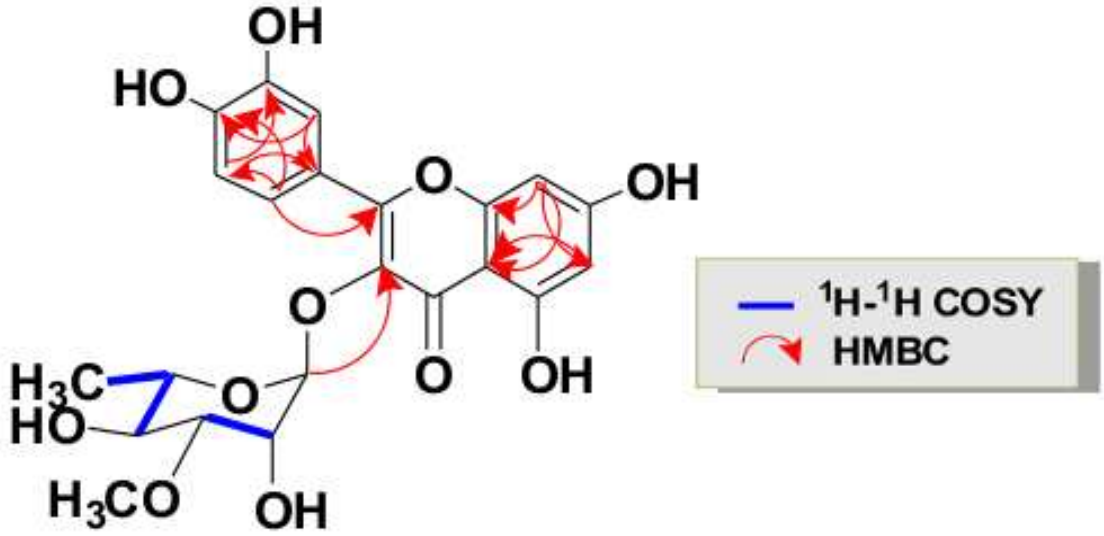

Figure 3.4: Key ^{1}H-^{1}H COSY and HMBC correlations observed for **6**

agreement with the quercetin skeleton bearing a carbonyl and two hydroxyl groups. In addition, four signals of OH hydrogens were observed at δ_H 12.63 (1H, s), 10.88 (1H, s), 9.71 (1H, s), and 9.34 (1H, s). The location of the sugar part, according to HMBC analysis (Figure 3.4), was shown to attach to the C-3 of aglycone. The small coupling constant (1.6 Hz) of the anomeric proton (δ_H 5.24) indicated its α configuration.[6]

Compound **7** (Figure 3.5) was isolated as a yellow amorphous solid and gave the molecular formula $C_{27}H_{30}O_{15}$, as deduced from HR-FABMS m/z 617.1584 (calcd for $C_{27}H_{30}O_{15}Na$, 617.1558). The proton signals showed two aromatic doublets at δ_H 6.20 and 6.39, and an ABX system at δ_H 7.66 ($J = 2$ Hz), 6.84 ($J = 8$ Hz), and 7.56 ($J = 2$ Hz and 8 Hz), confirming that the aglycone was quercetin. The ^{13}C NMR spectrum of **7** showed 27 resonances, including one methoxy group (δ_C 48.5) attached to one of the sugar moieties. Comparison of NMR spectral data of **7** differed from

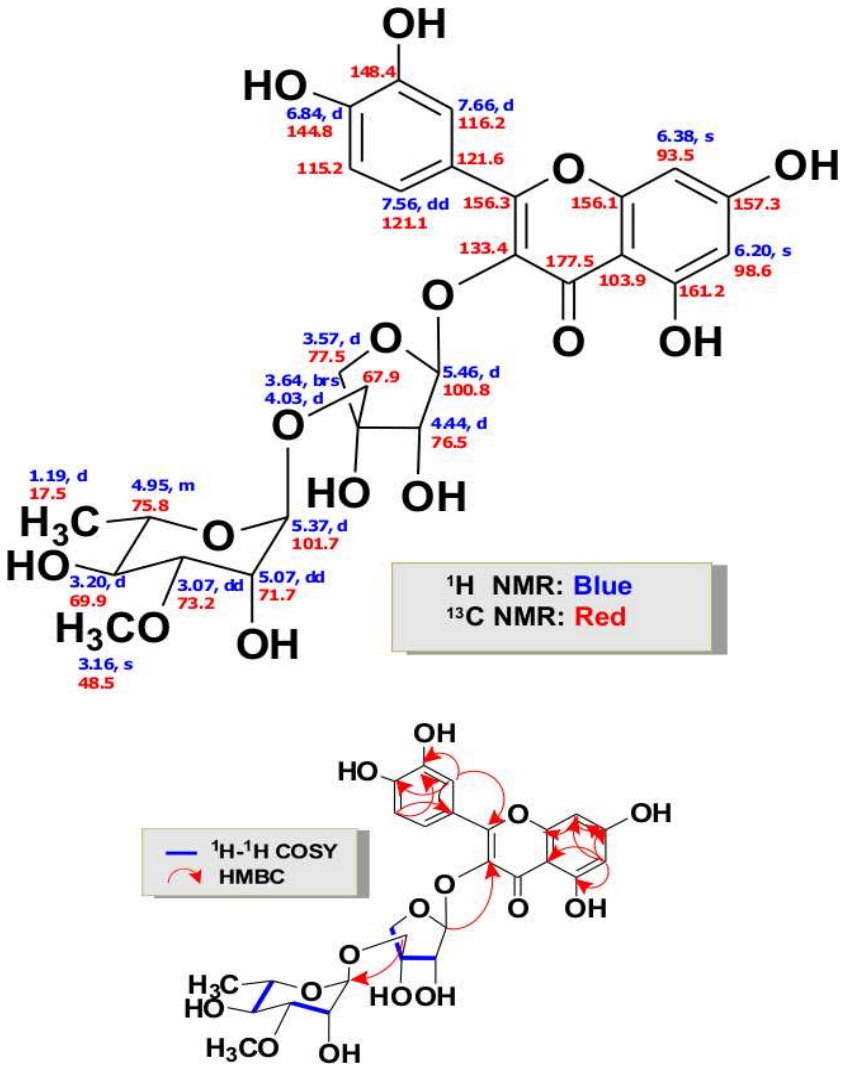

Figure 3.5: Structure of compound **7**, key ^{1}H-^{1}H COSY and HMBC correlations observed for **7**

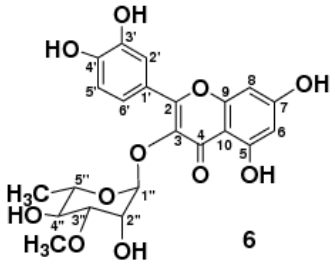

6

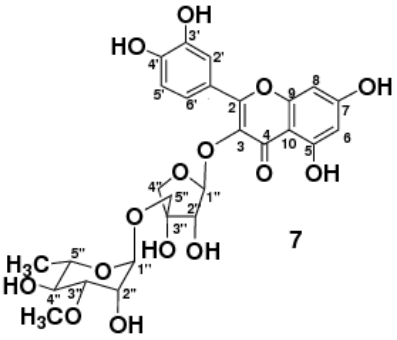

7

Table 3-1. ^{1}H and ^{13}C NMR spectral data of **6** and **7** (in DMSO-d_6)

Position	**6**		**7**	
	δ_H (J in Hz)	δ_C	δ_H (J in Hz)	δ_C
2		156.4		156.3
3		134.2		133.4
4		177.7		177.5
5		161.3		161.2
6	6.19 d (2.0)	98.6	6.20 d (2.0)	98.6
7		157.3		156.2
8	6.38 d (2.0)	93.6	6.39 d (2.0)	93.5
9		156.4		156.1
10		104.1		103.9
1'		120.7		121.6
2'	7.28 d (2.0)	115.6	7.66 d (2.0)	116.2
3'		148.4		148.4
4'		145.2		144.8
5'	6.86 d (8.0)	115.4	6.84 d (8.0)	115.2
6'	7.25 dd (2.0, 8.0)	121.1	7.56 dd (2.0, 8.0)	121.1
1"	5.24 d (1.6)	101.8	5.46 d (3.3)	100.8
2"	4.92 dd (1.6, 3.0)	70.5	4.44 d (3.3)	74.0
3"	3.12 dd (9.0, 3.0)	71.1	-	76.5
4"	3.50 d (9.0)	70.0	3.57 d (9.6) 3.57 d (9.6)	77.5
5"	4.70 m	70.3	4.02 d (8.0) 3.63 d (8.0)	67.9
6"	0.79 d (6.0)	17.5		
1'"			5.37 d (2.0)	101.7
2'"			5.07 dd (2.0, 1.2)	71.1
3'"			3.07 dd (8.0, 1.2)	73.2
4'"			3.20 d (8.0)	69.9
5"			4.95 m	75.8
6"			1.19 d (6.0)	17.5
4'"-OCH_3	3.15 s	48.6	3.16 s	48.5
5-OH	12.63 s			
7-OH	10.88 s			
3'-OH	9.34 s			
4'-OH	9.71 s			

6 in the sugar chain. Further HMBC analysis (Fig. 2) indicated the connections of sugar units between δ_H 5.46 (H-1") and δ_C 133.4 (C-3), and between δ_H 3.63 (H-5") and δ_C 101.7 (C-1"'). Acid hydrolysis and HPLC isolation gave quercetin, D-apiose and L-acofriose. The orientation of the anomeric proton of the first sugar (D-apiose, δ 5.46) was deduced as β since the coupling constant was smaller ($J = 3.3$ Hz)[7] than that of α ($J = 4.5$ Hz).[8] Furthermore, the small coupling constant observed for the anomeric proton of the second sugar (L-acofriose, δ_H 5.37, $J = 2.0$ Hz) suggested its α configuration.[6] The D-form of the first sugar connected to aglycone was confirmed by comparing its specific rotation $[\alpha]_D^{21}$ +6.1 (c 0.03, H_2O) with the reported values of an authentic sample, $[\alpha]_D^{22}$ +5.2 (c 1.1, H_2O).[9] The downfield location of the C-3"' absorption of the second sugar showed the presence of a methoxy group at C-3"'. The sugar was identified as 3-*O*-methyl-rhamnose and was confirmed as having an L-form by the same method as compound **6**.

3.2.2 Known Compounds

Quercitrin (**8**)[18]

^{1}H and ^{13}C NMR data, see Table 3-3, FAB MS m/z $[M + Na]^+$ 471

Afzelin (**9**)[19]

^{1}H and ^{13}C NMR data, see Table 3-3, FAB MS m/z $[M + Na]^+$ 455

Kaempferol-3-*O*-(2-*O*-acetyl-α-L-rhamnopyranoside (**10**)[20]

^{1}H and ^{13}C NMR data, see Table 3-3, FAB MS$m/z$ $[M + H]^+$ 475

Rutin (**11**)[21]

^{1}H and ^{13}C NMR data, see Table 3-4, FAB MS m/z $[M + Na]^+$ 633

Kaempferide 3-*O*-α-L-rhamnopyranoside (**12**)[22]

^{1}H and ^{13}C NMR data, see Table 3-4, FAB MS m/z $[M + K]^+$ 485

Kaempferol 3-*O*-α-L-arabinofuranoside (13)[23]

^{1}H and ^{13}C NMR data, see Table 3-4, FAB MS m/z $[M + Na]^+$ 441

3.3 Acivity Assay

Hh/GLI1 inhibitory effects of all isolated compounds (**6-13**) were further evaluated. Compounds **6**, **7** and **13** inhibited Hh/GLI-mediated transcriptional activity with IC_{50} values of 0.5, 19.1 and 2.0 μM, respectively, whereas compounds **8-12** were inactive (Figure 3.6 A, Table 3-2). In this assay, Gli1 protein expression was induced by 12-h treatment with tetracycline. Removal of tetracycline after another 12 h, followed by the addition of samples eliminated the undesired production of GLI1 via CMV promoter activation. Cell viability of compounds was checked simultaneously with luciferase activity under a fluorimetric microculture cytotoxicity assay (FMCA) system.[10] Of the 3 active compounds, compound **6** appeared to be the most potent Hh/GLI-1 inhibitor.

We further examined the cytotoxicity of active compounds against PANC1, DU145 and C3H10T1/2 using the FMCA system. The results revealed that compounds **6**, **7** and **13** were cytotoxic against PANC1 cells (IC_{50} values of 0.7, 20.0 and 1.8 μM, respectively) and DU145 cells (IC_{50} values of 0.8, 22.0 and 2.4 μM, respectively) but did not affect normal cell lines (Figure 3.6 B, Table 3-2). The cytotoxicity of **6**, **7** and **13** against PANC1 and DU145 cells may be associated with their Hh/GLI transcriptional activity inhibition.

To ensure that the inhibition of Hh signaling by **6** was associated with the expression of GLI-related proteins (PTCH and BCL-2) and to identify the effect of **6** on downstream events, we checked the protein levels of full, cytoplasmic and nuclear

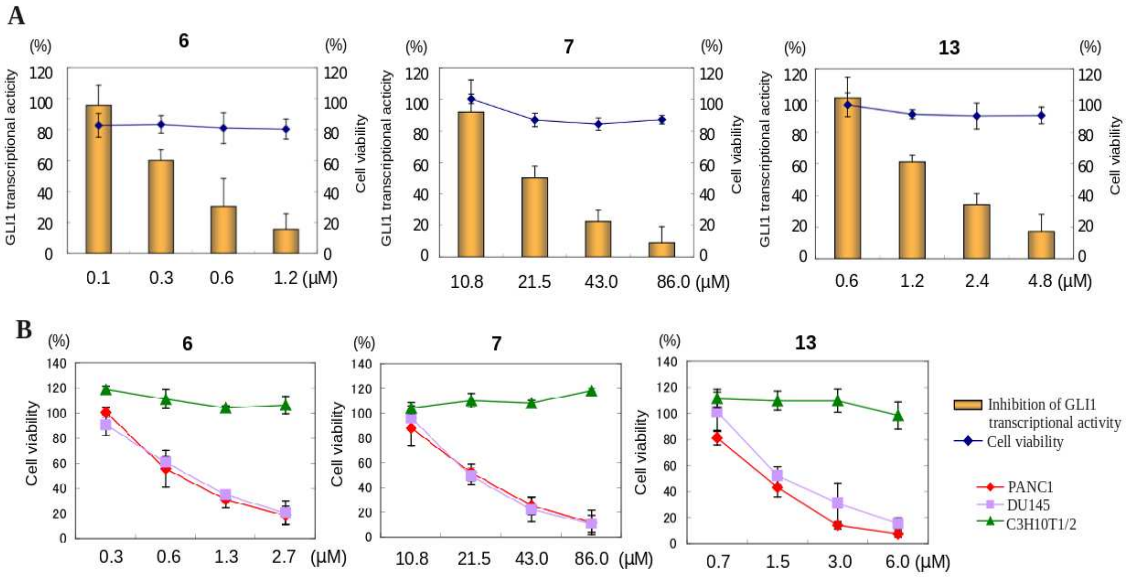

Figure 3.6: (A) Inhibition of GLI1-mediated transcriptional activity (solid columns) and cell viability (solid curves) of compounds **6**, **7** and **13**. HaCaT-GLI1-Luc cells were seeded onto a 96-well plate (2 x 10^5 cells per well) and then treated with compounds 12 h after tetracycline addition. Cell viability and luciferase activity were determined at the same time. (B) Cytotoxicity of compounds **6**, **7** and **13** against PANC1, DU145, and C3H10T1/2 cells. Assays were performed at 0.05 % DMSO (n=3). Error bars represent s.d.

PANC1 after treatment with **6**. As a result, **6** reduced the expression of PTCH and BCL-2 proteins in a dose-dependent manner. Our Western blot result also showed that treatment with **6** at a concentration of 1.6 μM led to a significant decrease in the protein level of nuclear GLI1 in PANC1 (Figure 3.7 A).

To further understand the molecular mechanism underlying the Hh signaling inhibitory effect of **6**, we checked the expression of a GLI-related gene (Ptch) using real-time quantitative RT-PCR. It has previously been suggested that Ptch is a repressive Hh receptor, and elevated expression of this gene results in the concomi-

Table 3-2. IC_{50} values (μM) of GLI-mediated transcriptional inhibition and cytotoxicity against cancer cells (PANC1, DU145) and C3H10T1/2 cells.

Compound	GLI transcriptional inhibition (IC_{50}, μM)	Cytotoxicity (IC_{50}, μM)		
		PANC1	DU145	C3H10T1/2
6	0.5	0.7	0.8	>100
7	19.1	20.0	22.0	>100
8	43.5	36.3	40.0	-
9	98.0	45.0	110.2	-
10	58.3	56.6	50.9	-
11	64.0	60.5	71.8	-
12	41.5	42.8	37.5	-
13	2.0	1.8	2.4	>100

tant expression of Hh target genes, including GLI1.[11] Consistent with this, our data showed that the downregulation of Ptch mRNA expression is essential for the inhibition of Hh/GLI1 signaling on PANC1 treated with **6** (Figure 3.7 B).

Loss of Ptch function has been reported to cause aberrant Hh signaling by Smo.[12] Most known Hh modulators, including cyclopamine, repress the pathway by antagonizing Smo activation; however, one of the oncogenic Smo mutants (SmoM2) is apparently resistant to cyclopamine[13] and most Smo inhibitors were not effective against medullablastoma and cancer associated with downstream lesions.[14]

To verify the function of Smo in PANC1 during the Hh inhibition of **6**, we knocked down Smo expression in PANC1 cells by siRNA and performed real-time quantitative RT-PCR on its mRNA expression. Transfection of a non-targeting siRNA at the same concentration served as a control. The transfection results, as confirmed by Western blotting, proved the total depletion of the Smo protein level after a silencing process (Figure 3.7 C, bottom panel). Accordingly, silencing of Smo siRNA significantly reduced the expression of Ptch mRNA expression in PANC1 cells treated with **6** (Figure 3.7 C, upper panel). These results thus indicated that **6** inhibited Hh signaling in an Smo-independent manner.

Because the inhibitory effect of **6** resulted in the decreased level of GLI1-related proteins (PTCH and BCL-2) as well as blocking GLI1 transcription factor translocation into the nucleus in PANC1 cells (Figure 3.7 A), we may speculate that this

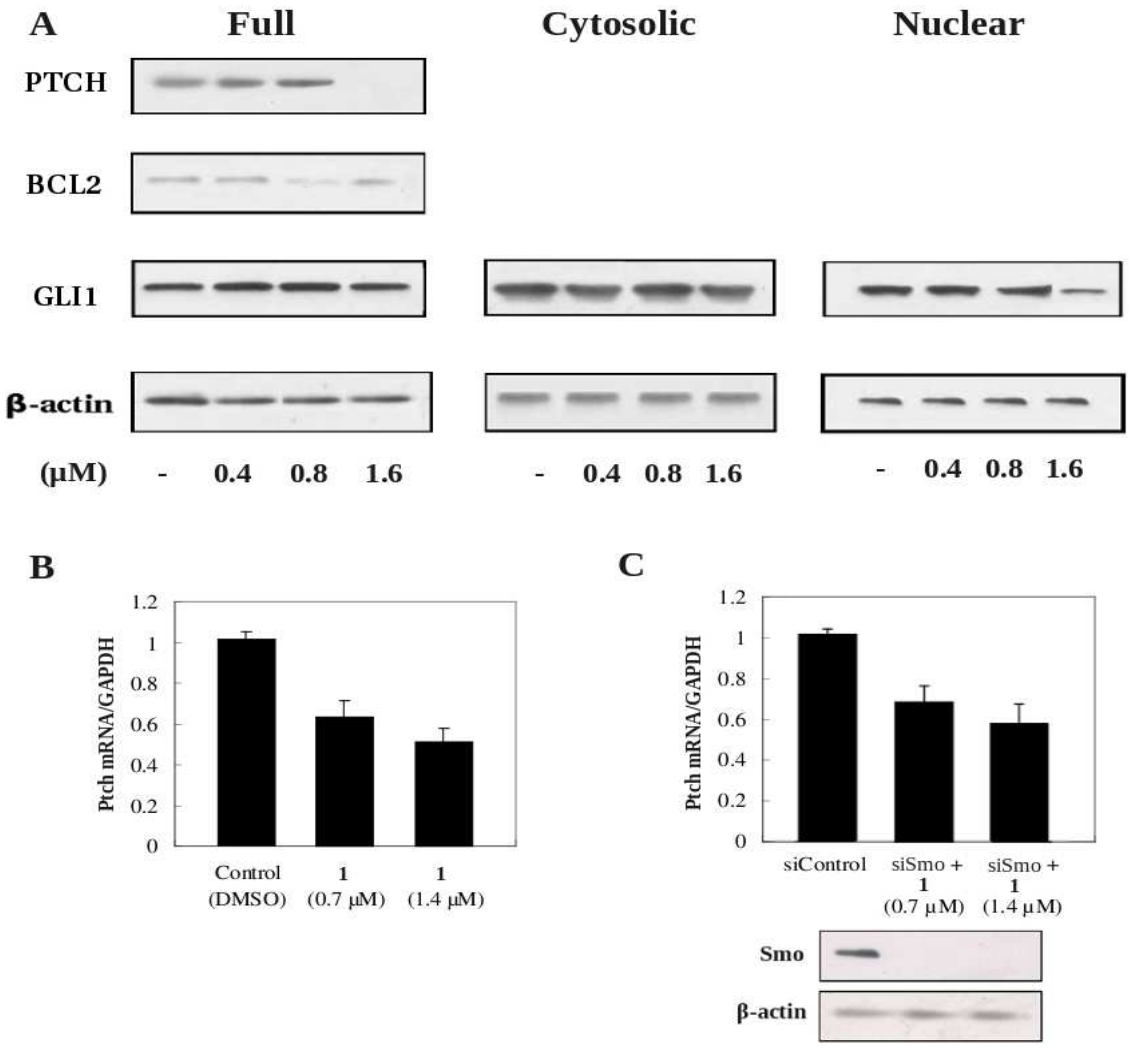

Figure 3.7: (A) Effect of compound **6** on GLI1 and/or GLI-related protein (PTCH and BCL2) levels in full, cytosolic and nuclear PANC1 cells. (B) Inhibition of Ptch mRNA expression by compound **6** in PANC1 cells. GAPDH was used as an internal control. Assays were performed at 0.05 % DMSO (n = 3). Error bars represent s.d. (C) Expression of Ptch mRNA (upper panel) and Smo protein (bottom panel) in PANC1 treated with **6** after siRNA-mediated silencing of Smo.

compound antagonizes GLI1 activator function. In accordance with this result, several reports have previously described that GLI function can be modulated without Smo interference via numerous types of GLI signaling, such as transforming growth factor- (TGF),[15] mitogen-activated protein kinase (MAPK)[16] and posphatidylinositol 3-kinase (PI3K)/Akt signaling.[17]

In conclusion, we have isolated naturally occurring Hh/GLI inhibitors including 2 new compounds (**6**-**7**) from *Excoecaria agallocha*. Compound **6** inhibited the translocation of GLI1 transcription factor into the nucleus of PANC1. Quantitative RT PCR of **6** exhibited that the reduction of Hh signaling was not caused by Smo interference, but rather by other unrevealed mechanisms related to the GLI1 inhibitory function. This is the first report of an Hh/GLI signaling inhibitor which reduces the level of GLI1 in the nucleus.

3.4 Acid Hydrolysis

Compounds **6** (4 mg) and **7** (1.5 mg) were respectively reacted in 6 mL and 3 mL of 5 % H_2SO_4 for 1 hour at 95^0C. Five drops of water were added and then each mixture was partitioned with EtOAc three times. The EtOAc layer was washed with saturated aqueous $NaHCO_3$ and H_2O, dried over Na_2SO_4 and concentrated. Aglycones of **6** (2 mg) and **7** (0.6 mg) were identical to quercetin by comparing the NMR data with the literature. The H_2O-soluble part of **6** was purified by Amberlite IRA 96 SB AG (10 x 210 mm; eluent, H_2O) to give the sugar part (1.8 mg). Sugar of **7** was purified by reverse-phase HPLC (CAPCELL PACK 4.6 x 250 mm; eluent H_2O/MeOH=15/85, flow rate 1 mL/min, detection UV at 232 nm) to give D-apiose (*t*R 5.0 min, 0.3 mg) and L-acofriose (*t*R 18.5 min, 0.4 mg).

References

1. Zou, J. H.; Dai, J. .; Chen, X.; Yuan, J. Q. *Chem. Pharm. Bull.* **2006**, *54*, 920-921.

2. Konoshima, T.; Konishi, T.; Takasaki, M.; Yamazoe, K.; Tokuda, H. *Biol. Pharm. Bull.* **2001**, *24*, 1440-1442.

3. Ericson, K. L.; Beutler, J. A.; Cardellina, J. H.; McMahon, J. B.; Newman, J. D.; Boyd, M. R. *J. Nat. Prod.* **1995**, *58*, 769-772.

4. Konishi, T.; Yamazoe, K.; Kanzato, M.; Konoshima, T.; Fujiwara, Y. *Chem. Pharm. Bull.* **2003**, *51*, 1142-1146.

5. Muhr, H.; Hunger, A.; Reichstein, T. *Helv. Chim. Acta* **1954**, *31*, 403.

6. Yamauchi, T.; Abe, F.; Wan, A. S. C. *Chem. Pharm. Bull.* **1987**, *35*, 2744-2749.

7. Kanchanapoom, T.; Kasai, R.; Yamasaki, K. *Phytochemistry* **2002**, *59*, 557-563.

8. Lei, Y.; Wu, L. J.; Shi, H. M.; Tu, P. F. *Helv. Chim. Acta* **2008**, *91*, 495-500.

9. Ho, P. T. *Can. J. Chem.* **1979**, *57*, 381-383.

10. Larsson, R.; Kristensen, J.; Sandberg, C.; Nygren, P. *Int. J. Cancer* **1992**, *50*, 177-185.

11. Lauth, M.; Bergstrm, A.; Shimokawa, T.; Toftgrd, R. *Proc. Natl. Acad. Sci. U.S.A.***2007**, *104*, 8455-8460.

12. Carpenter, D.; Stone, D. M.; Brush, J.; Ryan, A.; Armanini, M.; Frantz, G.; Rosenthal, A.; de Savauge, F. J. *Proc. Natl. Acad. Sci. U.S.A.* **1998**, *95*, 13630-13634.

13. Taipale, J.; Chen, K. K.; Cooper, M. K.; Wang, B.; Mann, R. K.; Milenkovic, L.; Scott, M. P.; Beachy, P. A.*Nature* **2000**, *406*, 1005-1008.

14. Lee, Y.; Kawagoe, R.; Sasai, K.; Li, Y.; Russell, H. R.; Curran, T.; McKinnon, P. *J. Oncogene* **2007**, *26*, 6442-6447.

15. Dennler, S.; Andr, J.; Alexaki, I.; Li, A.; Magnaldo, T.; Dijke, P.; Wang, X.; Verrechia, F.; Muviel, A. *Cancer Res.* **2007**, *67*, 6981-6986.

16. Riobo, N. A.; Haines, G. M.; Emerson, C. P. Jr. *Cancer Res.* **2006**, *66*, 839-845.

17. Riobo, N. A.; Lu, K.; Ai, X.; Haines, G. M.; Emerson, C. P. Jr. *Proc. Natl. Acad. Sci. U.S.A.* **2006**, *103*, 4505-4510.

18. Peng, F. Z.; Strack, D.; Baumert, A.; Subramaniam, R.; Goh, N. K.; Chia, T. F.; Tan, S. N.; Chia, L. S. *Phytochemistry* **2003**, *62*, 219-228.

19. Matthes, H. W. D.; Luu, B.; Ourrison, G. *Phytochemistry* **1980**, *19*, 2643-2650.

20. Masuda, T.; Jitoe, A.; Kato, S.; Nakatani, N. *Phytochemistry* **1991**, *30*, 2391-2392.

21. Wooten, J. B.; Kalengamaliro, N. E.; Axelson, D. E. *Phytochemistry* **2009**, *70*, 940-951.

22. Bilia, A. R.; Palme, E.; Marsill, A.; Pistelli, L.; Morelli, I. *Phytochemistry* **1993**, *32*, 1078-1079.

23. Kumar, N.; Singh, B.; Kaul, V. K. *Nat. Prod. Commun.* **2006**, *1*, 623-626.

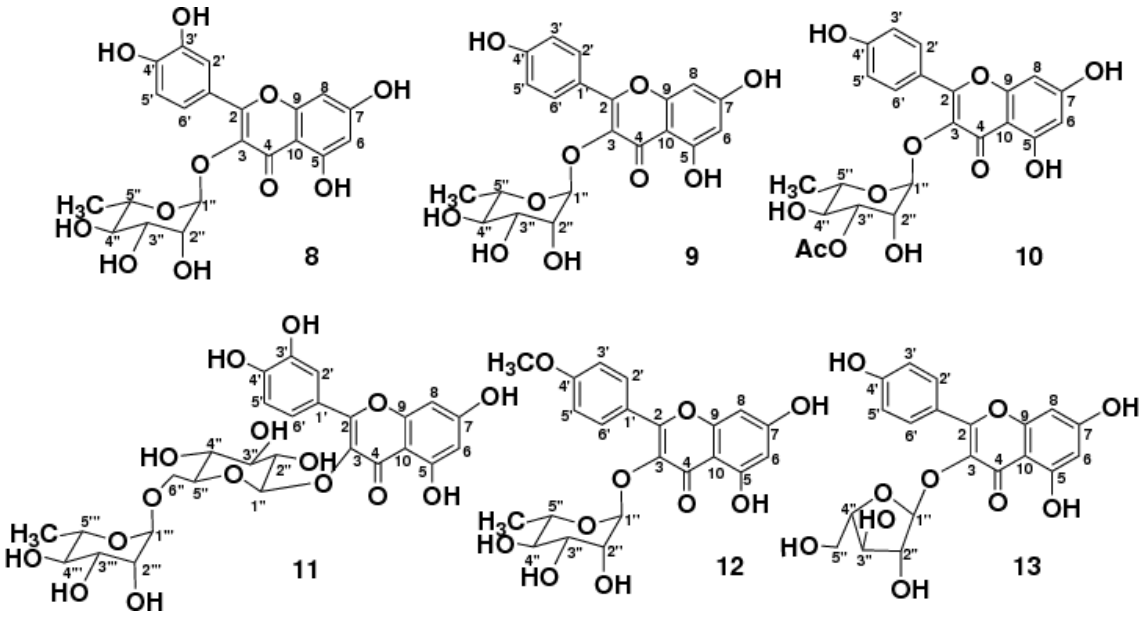

Figure 3.8: Structures of Compounds **8-13**

Table 3-3. NMR Spectroscopic data for **8-10** (in DMSO-d_6)

	Compound **8**		Compound **9**		Compound **10**	
Position	δ_C	δ_H (J in Hz)	δ_C	δ_H (J in Hz)	δ_C	δ_H (J in Hz)
2	158.6		158.4		157.2	
3	136.2		135.7		130.6	
4	179.6		179.2		177.7	
5	163.2		164.9		161.2	
6	99.9	6.19 (1H, d, 2)	99.5	6.26 (1H, d, 2)	98.7	6.19 (1H, s)
7	166.1		164.9		164.3	
8	94.7	6.36 (1H, d, 2)	94.5	6.46 (1H, d, 2)	93.7	6.40 (1H, s)
9	159.3		157.9		159,9	
10	105.8		105.8		104.1	
1'	122.9		122.6		120.4	
2'	116.4	7.33 (1H, d, 2)	131.7	7.86 (1H, d, 8.5)	134.2	7.85 (1H, d, 8)
3'	146.4		116.2	7.01 (1H, d, 8.5)	115.4	7.73 (1H, d, 8)
4'	149.8		160.8		160.9	
5'	116.9	6.91 (1H, d, 8)	159.9	7.01 (1H, d, 8.5)	156.5	7.75 (1H, d, 8)
6'	122.8	7.29 (1H, d, 8)	160.7	7.86 (1H, d, 8.5)	160.9	7.85 (1H, d, 8)
1"	103.6	5.34 (1H, d, 2)	102.6	5.53 (1H, d, 2)	101.7	5.27 (1H, d, 2)
2"	72.0	4.21 (1H, dd, 2, 3)	71.4	4.21 (1H, dd, 2, 3)	70.6	4.97 (1H, br, s)
3"	72.1	3.75 (1H, dd, 9, 3)	72.0	3.69 (1H, dd, 3, 9)	71.1	3.12 (1H, dd, 9, 3)
4"	73.2	3.41 (1H, d, 9)	72.9	3.35 (1H, dd, 9. 8)	70.0	3.64 (1H, d, 9)
5"	71.9	3.34 (1H, m)	71.3	3.30 (1H, d, 8)	70.3	4.74 (1H, m)
6"	17.7	0.93 (1H, d, 6)	17.7	0.90 (3H, d, 6)	17.4	0.78 (3H, d, 6)
5-OH				12.71 (br, s)		12.62 (br, s)
2"-OAc					170.3	
					20.7	1.98 (3H, s)

Table 3-4. NMR Spectroscopic data for **11-13** (in DMSO-d_6)

	Compound **11**		Compound **12**		Compound **13**	
Position	δ_C	δ_H (*J* in Hz)	δ_C	δ_H (*J* in Hz)	δ_C	δ_H (*J* in Hz)
2	159.3		159.0		156.5	
3	136.2		133.5		133.2	
4	179.6		179.4		177.4	
5	165.9		163.0		161.1	
6	99.8	6.19 (1H, d, 2)	99.8	6.20 (1H, d, 2)	98.9	6.13 (1H, d, 2)
7	163.2		165.7		157.7	
8	94.7	6.36 (1H, d, 2)	95.0	6.88 (1H, d, 2)	93.8	6.36 (1H, d, 2)
9	158.5		158.7		156.4	
10	104.6		104.5		103.5	
1'	122.8		12.8		120.7	
2'	116.1	7.33 (1H, dd, 2)	131.8	8.06 (1H, d, 8)	130.7	8.00 (1H, d, 8)
3'	146.4		114.3	7.10 (1H, d, 8)	115.3	6.85 (1H, d, 8)
4'	149.7		163.0		159.9	
5'	116.4	6.91 (1H, dd, 2, 8)	114.3	7.10 (1H, d, 8)	115.4	6.85 (1H, d, 8)
6'	122.9	7.29 (1H, dd, 2, 8)	132.0	8.06 (1H, d, 8)	128.4	8.00 (1H, d, 8)
1"	105.9	5.16 (1H, d, 6.6)	102.4	5.37 (1H, d, 3)	107.9	5.59 (1H, 0.8)
2"	74.1	3.58 (1H, m)	71.8	4.21 (1H, d, 3)	82.1	4.12 (1H, br, s)
3"	78.1	3.41 (1H, m)	72.0	3.70 (1H, dd, 9, 3)	77.1	3.70 (1H, m)
4"	71.9	3.62 (1H, m)	73.5	3.39 (1H, d, 9)	86.3	3.39 (1H, m)
5"	75.7	3.89 (1H, m)	71.0	3.35 (1H, m)	60.8	3.35 (1H, dd, 9, 6)
6”	66.9	3.69 (1H, dd, 8, 3) 3.30 (1H, m)	17.9	0.91 (3H, d, 6)		3.31 (1H, dd, 9, 6)
1"'	103.5	5.34 (1H, br, s)				
2"'	71.9	4.21 (1H, br, s)				
3"'	73.2	3.35 (1H, dd, 9. 3)				
4"'	69.1	3.69 (1H, d, 9)				
5"'	72.02	4.05 (1H, m)				
6"'	17.6	0.90 (3H, d, 6)				
4"-OCH_3	49.8	3.32 (3H, s)				

Chapter 4

Separation of *Vallaris glabra*

Vallaris glabra Kuntz. (apocynaceae) (Figure 4.1) is well known to the natives of Thailand and locally named as *bread flowers*. Its phytochemical study revealed the presence of monoterpenes, sequiterpenes and acyclic monoterpene alcohols.[1] No papers reported about the potential therapeutical use of the plant.

4.1 Extraction and Isolation

The MeOH extract (10.0 g) of dried leaves of *Vallaris glabra* was partitioned between hexane, EtOAc, and BuOH. The EtOAc extract (817.1 mg) was subjected to silica gel PSQ100B column chromatography (30 x 350 mm) and eluted successively with a hexane-EtOAc solvent system (8:1 to 1:1) to yield 8 fractions (1A to 1H). Fraction 1H (51 mg) was chromatographed over silica gel PSQ100B (12 x 250 mm), using a hexane-EtOAc solvent system to afford compound **14** (6.0 mg). Another active fraction from the EtOAc extract (fraction 1G, 44 mg) underwent ODS flash chromatography (12 x 245 mm), eluted with increasing MeOH (30-100 %) in H_2O to give compound **15** (1.0 mg).

Figure 4.1: *Vallaris glabra*

4.2 Structure Elucidation

One new compound (**15**) and one known compound (**14**) were isolated from *Vallaris glabra* (Figure 4.2). The structure elucidation of known compound, acoschimperoside P, 2'-acetate (**14**), was on the basis of comparison with spectral data of the reported values.[2]

4.2.1 Known Compound

Acoschimperoside P, 2'-acetate (**14**)

^{1}H and ^{13}C NMR data, see Table 3-4, FAB-MS m/z $[M + Na]^{+}$ 657

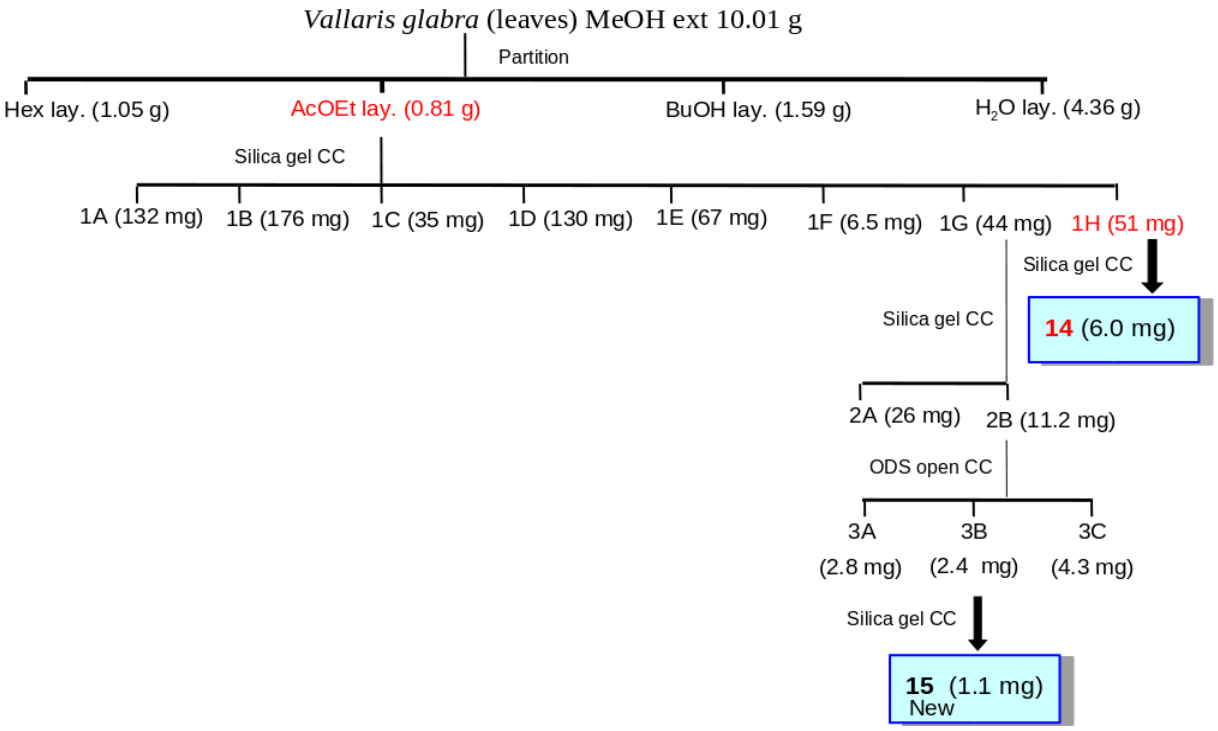

Figure 4.2: Isolation Scheme of *Vallaris glabra*

4.2.2 New Compound

Compound **15** (Figure 4.3) was obtained as a pale yellow powder and had a molecular weight at m/z 657.3353 ([M+Na]$^+$, Δ-1.3 mmu), corresponding to the molecular formula of $C_{34}H_{50}O_{11}$ in the HR-FABMS. The IR absorption bands suggested the presence of hydroxyl (3395 cm^{-1}) (br) and carbonyl (1733 cm^{-1}) groups. The UV absorption maxima were at UV (MeOH) λ max 216 nm (log ϵ 3.8) and 275 nm (log ϵ 2.1). Spectral data of compound **15** showed three ester C=O groups (δ_C 173.7; δ_C 169.8; δ_C 169.5), olefin (δ_H 6.31; δ_C 121.2, 170.3), and an oxygenated CH_2 (δ_H 5.43, 5.27; δ_C 75.8) (Fig. 1, Table 1). Acid hydrolysis gave D-acofriose, whose D form was identified by comparison of $[\alpha]_D^{20}$ -28.4 (c 0.1, MeOH) with the literature (-27.0).[3] The α configuration of D acofriose was assigned based on the downfield

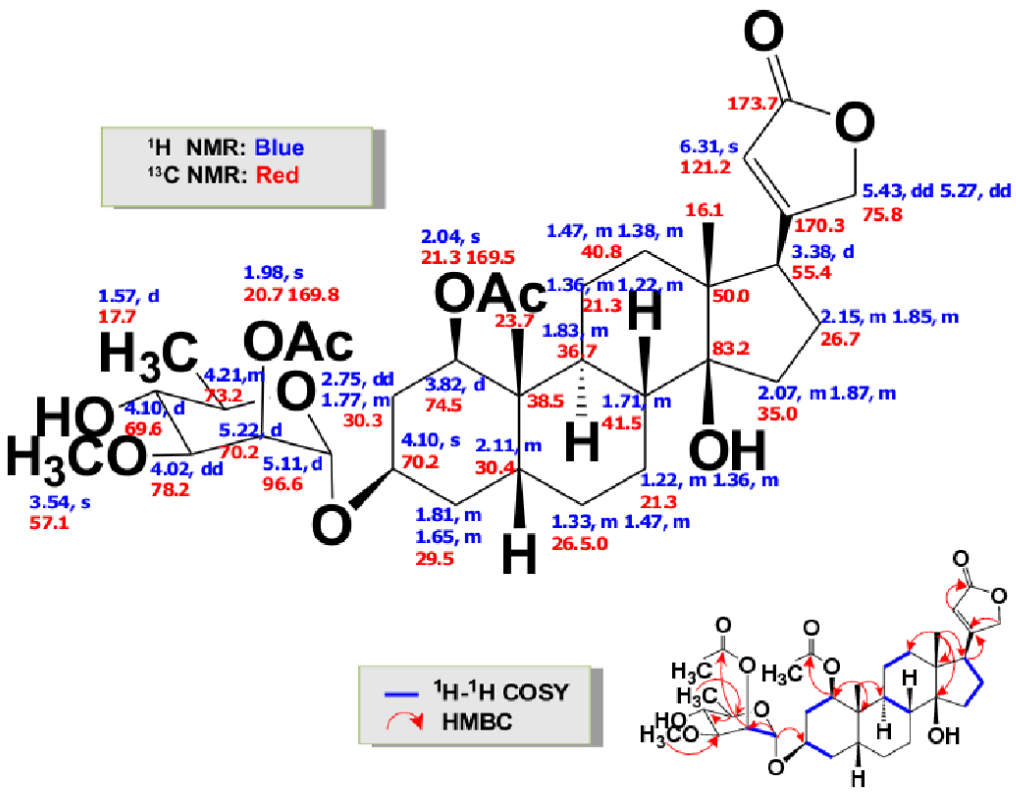

Figure 4.3: Structure of Compound **15**, key ^{1}H-^{1}H COSY and HMBC correlations observed for **15**

chemical shift of its anomeric proton (δ_H 5.11).[4,5] The sugar part was attached to the O-atom at C-3 of the aglycone on the basis of an HMBC correlation between the anomeric H-atom and C-3 at the δ_C 70.2 (Figure 4.3).

4.3 Activity Assay

The Hh/GLI inhibitory effect of compounds **14** and **15** were further evaluated. Compound **14** inhibited Hh/GLI-mediated transcriptional activity with IC_{50} value of 2.3 μM (Figure 4.4, Left), whereas compound **15** was inactive (data is summarized

in Table 4-1). Compound **14** was cytotoxic against PANC1 cells (IC_{50} value of 3.6 μM) and DU145 cells (IC_{50} value of 1.8 μM) but less affect a normal cell line (Figure 4.4, Right). This cytotoxicity effect may be associated with the ability of compound **14** to inhibit Hh/GLI1 signaling pathway. Similar type of cardiac glycosides, isolated from *Adenium obesum*, were previously also identified as Hh inhibitors.[8]

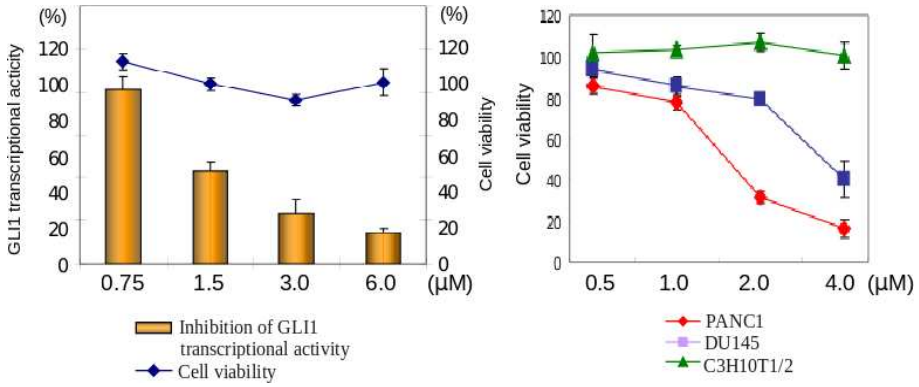

Figure 4.4: (Left) Inhibition of GLI1-mediated transcriptional activity (solid columns) and cell viability (solid curves) of compounds **14**. HaCaT-GLI1-Luc cells were seeded onto a 96-well plate (2 x 10^5 cells per well) and then treated with compounds 12 h after tetracycline addition. Cell viability and luciferase activity were determined at the same time. (Right) Cytotoxicity of compounds **14** against PANC1, DU145, and C3H10T1/2 cells. Assays were performed at 0.05 % DMSO (n=3). Error bars represent s.d.

To ascertain whether the inhibition of Hh signaling by **14** was associated with the expression of GLI-related proteins (PTCH and BCL-2), protein lysates of PANC1-treated with **14** was blotted and analyzed. Reduced expression of PTCH and BCL-2 proteins in a concentration-dependent fashion, as confirmed by western blot analysis, suggesting that the block of Hh signaling inhibited the expression of tumor suppressor and antiapoptosis proteins (Figure 4.5).

In conclusion, two cardiac glycosides were isolated from the leaves of *Vallaris glabra*.

Table 4-1. IC_{50} values (μM) of GLI-mediated transcriptional inhibition and cytotoxicity against cancer cells (PANC1, DU145) and C3H10T1/2 cells.

Compound	GLI transcriptional inhibition (IC_{50}, μM)	Cytotoxicity (IC_{50}, μM)		
		PANC1	DU145	C3H10T1/2
14	2.3	3.6	1.8	>25.0
15	28.9	20.3	22.1	>17.4

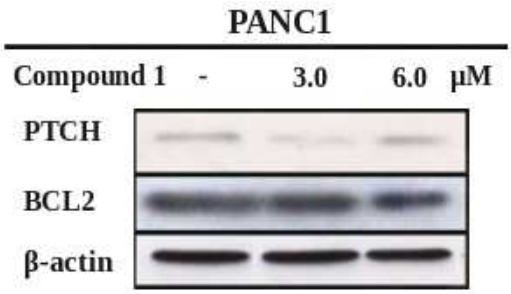

Figure 4.5: Inhibition of GLI-related protein (PTCH and BCL2) levels by compound **14** in PANC1 cells.

Compound **14** but not **15** was active in the assay for Hh signaling inhibition. In further experiments, compound **14** showed a strong cytotoxicity against human pancreatic (PANC1) and human prostate (DU145) cancer cells. The expression of GLI-related proteins (PTCH and BCL-2) according to a dose-dependent manner were also inhibited by **14**.

4.4 Acid Hydrolysis

Compound **15** (1.0 mg) in 5 % aq.HCl (1.5 mL) was heated at 95 ^{o}C for 1 hour. After cooling to room temperature, H_2O was added then extracted with EtOAc (x 3). The aqueous layer was neutralized with 10 % aqueous Na_2CO_3 solution (2 mL). Aglycone of **15** (0.5 mg) was identical to aglycone of acovenoside B by comparing the NMR data with the literature.[6] Sugar part of **15** (D-acofriose, 0.4 mg) was

identified based on R_F and α_D values of references.[3,7] Thin-layer chromatography (TLC) was performed on aluminium sheets coated with kieselgel (silica gel, type 60 F_{254}, Merck), $R_F = 0.72$ (EtOAc/MeOH, 2:1). $[\alpha]_D^{20}$ -28.4 (*c* 0.1, MeOH) (lit.-27.0).[3]

References

1. Wongpornchai, S.; Sriseadka, T.; Choonvisase, S. *J. J Agric Food Chem.* **2003**, *51*, 457-462.

2. Kaufmann, H. *Helvetica Chimica Acta* **1965**, *48*, 83-94.

3. Morrison, I. M.; Young, R.; Perry, M. B.; Adams, G. A. *Can J Chem.* **1967**, *45*, 1987-1990.

4. Kasai, R.; Okihara, M.; Asakawa, J.; Mizutani, K.; Tanaka, O. *Tetrahedron* **1979**, *35*, 1427-1432.

5. Popper, Z. A.; Sadler, I. H.; Fry, S. C.; *Biochemical Systemic and Ecology* **2004**, *32*, 279-289.

6. Hanna, A. G.; Elgamal, M. H. A.; Hassan, A. Z.; Duddeck, H.; Simon, A.; Kovacs, J.; Toth, G. *Magn Reson Chem.* **1998**, *36*, 936-942.

7. Kaufmann, H.; Mhlradt, P.; Reichstein, T. *Helvetica Chimica Acta* **1967**, *50*, 2280-2287.

8. Arai, M. A.; Tateno, C.; Koyano, T.; Kowithayakorn, T.; Kawabe, S.; Ishibashi, M. *Org. Biomol. Chem.* **2011**, *9*, 1133-1139.

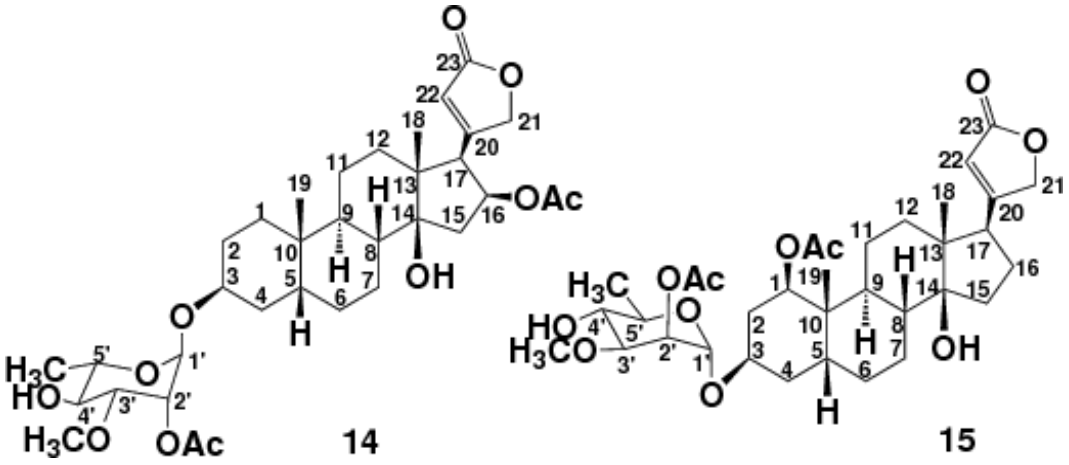

Figure 4.6: Structures of Compounds **14-15**

Table 4-2 ^{1}H and ^{13}C NMR spectral data of **14** and **15** (in Pyridine-d_5)

Position	**14**		**15**	
	δ_H (J in Hz)	δ_C	δ_H (J in Hz)	δ_C
1	1.53 m 1.57 m	30.8	3.82 d (4.6)	74.5
2	1.20 m 1.56 m	26.5	1.77 m 2.75 dd (9.0, 15.0)	30.3
3	4.15 brs	73.3	4.10 brs	70.2
4	1.74 m 1.98 m	30.1	1.81 m 1.65 m	29.5
5	1.51 m	35.6	2.11 m	30.4
6	1.32 m 1.43 m	24.0	1.33 m 1.47 m	26.5
7	1.66 m 1.30 m	21.4	1.22 m 1.36 m	21.3
8	1.78 m	42.0	1.71 m	41.5
9	1.81 m	37.1	1.83 m	36.7
10		35.1		38.5
11	1.30 m 1.66 m	21.0	1.36 m 1.22 m	21.3
12	1.43 m 1.32 m	38.7	1.47 m 1.33 m	40.8
13		50.4		50.0
14		83.2		82.9
15	2.78 dd (5.5, 9.7) 2.12 brs	41.2	2.07 m 1.87 m	35.0
16	5.68 dd (9.7. 8.9)	74.8	2.15 m 1.85 m	26.7
17	3.38 d (8.9)	56.7	3.38 d (8.9)	55.4
18	1.07 s	16.3	1.05 s	16.1
19	0.85 s	23.8	0.87 s	23.7
20		170.5		170.3
21	5.41 dd (1.7, 18.1) 5.54 dd (1.7, 18.1)	76.4	5.43 dd (1.0, 18.3) 5.27 dd (1.0, 18.3)	75.8
22	6.35 s	121.6	6.31 s	121.2
23		174.5		173.7
OAc	2.01 s	21.6 170.5	2.04 s	21.3 169.5
1'	5.23 d (1.7)	96.9	5.11 d (1.2)	96.6
2'	5.26 dd (1.7, 3.0)	70.1	5.22 dd (1.2, 2.8)	70.2
3'	4.01 dd (3.0, 9.0)	80.7	4.02 dd (2.8, 9.0)	78.2
4'	4.28 d (9.0)	69.1	4.10 d (9.0)	69.6
5'	4.15 m	72.5	4.21 m	73.2
6'	1.61 d (6.1)	18.3	1.57 d (6.3)	17.7
3'-OMe	3.55 s	57.6	3.54 s	57.1
2'-OAc	1.83 s	20.6 170.5	1.98 s	20.7 169.8

Chapter 5

Separation of *Ocimum gratissimum*

Ocimum gratissimum L (Lamiaceae) (Figure 5.1) commonly known as *alfavaca* is naturally used in treatment of different diseases, for example upper respiratory infections, diarrhea, headache, fever, ophtalmic, skin disease.[1] Volatile oil and chromenes have been isolated from this species, and have been reported to have anthelmintic effect.[2]

5.1 Extraction and Isolation

The chlorophyll free fraction (9.81 g) of extract, suspended in 10 % aq. MeOH, was partitioned x 3 with hexane, EtOAc and BuOH sucessively to give 1.82 g hexane extract. This active extract was separated by chromatography on silica gel 60 N (50 x 280 mm) with increasing amounts of EtOA in Hexane as eluent to afford fraction 2A-2E. Fraction 2B and 2C were pure compounds and have identified as compound **16** (5.74 mg) and **17** (25.9 mg). Fraction 2A (981 mg) was further underwent ODS open column chromatography (50 x 250 mm) to give fraction 3A-3K. Separation of

Figure 5.1: *Ocimum gratissimum*

fraction 3D (18.2 mg) on silica gel column chromatography yielded compounds **18** (8.2 mg), **19** (5.4 mg), and **20** (3.1 mg). Fraction 3F (51.6 mg) was subjected to preparative HPLC [Capcell Pack C.18 type Acr, 6 x 250 mm; MeOH : H_2O (3 :1); flow rate: 1.7 mL/min; RI and UV detection at 254 nm] to obtain compound **21** (2.1 mg). Fraction 4D (19.1 mg), afforded from the separation of fraction 3E (130.5 mg), was subjected to ODS open column chromatography (30 x 180 mm) to give compound **22** (2.2 mg), **23** (6.2 mg), **24** (1.2 mg), **25** (0.8 mg), **26** (2.0 mg), **27** (1.5 mg), and **28** (5.0 mg) (Figure 5.2).

5.2 Structure Elucidation

Three type of compounds were isolated from *Ocimum gratissimum* including chromenes which were commonly isolated. Triterpenes and flavones, however, were the first iso-

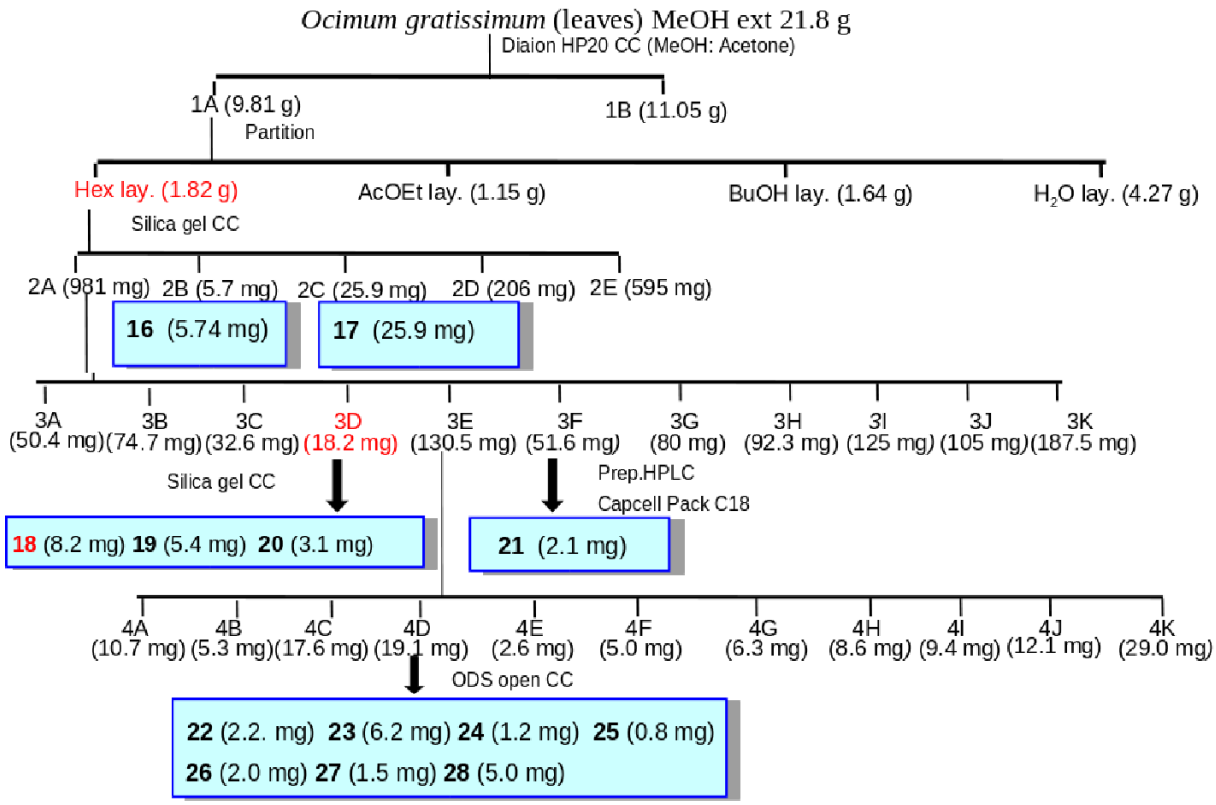

Figure 5.2: Isolation Scheme of *Ocimum gratissimum*

lated from this flowering type plant. Isolated compounds (**16-28**) were identified by comparing their spectroscopic data to literature values.

2β,19α -Glutin-7,21-diene-2,19-diol (**16**)[3]

^{1}H and ^{13}C NMR data, see Table 5-1, ESIMS m/z [M + Na]$^+$ 477

Friedoolean-8-en-3-ol-8, 29-diene (**17**)[4]

^{1}H and ^{13}C NMR data, see Table 5-1, ESIMS m/z [2M + Na]$^+$ 899

6-(1-methoxyethyl)-5,7-dimethoxy-2,2-dimethylchromene (**18**)[5]

^{1}H and ^{13}C NMR data, see Table 5-2, ESIMS m/z [M + Na]$^+$ 301

6-(1-methoxyethyl)-7-methoxy-2,2-dimethylchromene (**19**)[6]

^{1}H and ^{13}C NMR data, see Table 5-2, ESIMS *m/z* [2M + Na]$^{+}$ 519

6-(1-hydroxyethyl)-7-methoxy-2,2-dimethylchromene (**20**)[6]

^{1}H and ^{13}C NMR data, see Table 5-2, ESIMS *m/z* [M + Na]$^{+}$ 257

Evodione (**21**)[5]

^{1}H and ^{13}C NMR data, see Table 5-2, EIMS *m/z* [M + Na]$^{+}$ 285

Precocene (**22**)[7]

^{1}H and ^{13}C NMR data, see Table 5-2, EIMS *m/z* [M + Na]$^{+}$ 243

5,7,2'-trimethoxy-3',4'-methylendioxyflavone (**23**)[8]

^{1}H and ^{13}C NMR data, see Table 5-3, FAB-MS *m/z* [M + H]$^{+}$ 357

5,6,7,8,3',4',5'-heptamethoxy-flavone (**24**)[9]

^{1}H and ^{13}C NMR data, see Table 5-3, ESIMS *m/z* [M + Na]$^{+}$ 455

5,6,7,3',4',5'-hexamethoxy-flavone (**25**)[8]

^{1}H and ^{13}C NMR data, see Table 5-3, ESIMS *m/z* [M + Na]$^{+}$ 425

5,6,7,2'-tetramethoxy-3',4'-methylendioxyflavone (**26**)[8]

^{1}H and ^{13}C NMR data, see Table 5-3, FAB-MS *m/z* [M + H]$^{+}$ 387

Eupalestin (**27**)[9]

^{1}H and ^{13}C NMR data, see Table 5-3, ESIMS *m/z* [M + Na]$^{+}$ 439

f5,6,2',5',6'-pentamethoxy-3',4'-methylendioxyflavone (**28**)[1]0

^{1}H and ^{13}C NMR data, see Table 5-3, FAB-MS *m/z* [M + H]$^{+}$ 417

5.3 Activity Assay

The isolated compounds (**16-28**) were tested in the inhibition of GLI-mediated transcriptional activity and data is summarized in Table 5-4. Compound **18** showed moderate inhibition of GLI-mediated transcriptional activity, evidenced by the IC_{50} value of 10.0 μM (Figure 5.3, Left, Table 5-4). This compound was cytotoxic against cancer cells (PANC1 and DU145), in which Hh signaling is aberrantly activated (Figure 5.3, Right, Table 5-4). This result was in agreement with a significant reduction of the expression of anti-apoptosis BCL-2 and tumor suppressor PTCH in PANC1 after the treatment of **18** in a concentration-dependent manner (Figur 5.4).

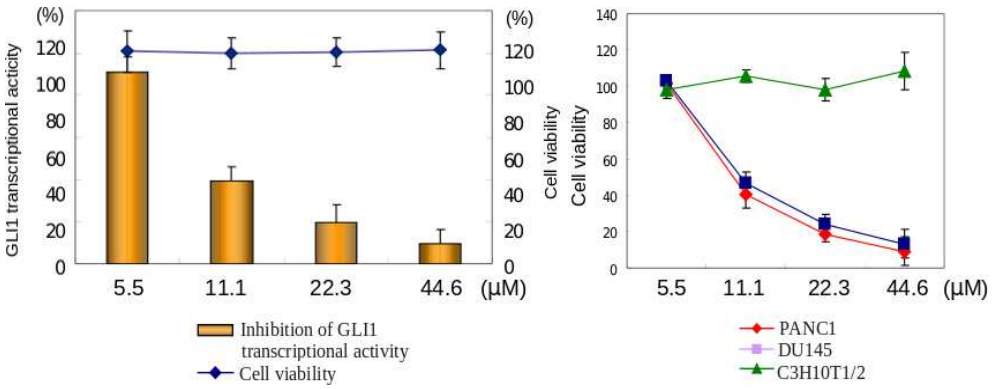

Figure 5.3: (Left) Inhibition of GLI1-mediated transcriptional activity (solid columns) and cell viability (solid curves) of compounds **18**. HaCaT-GLI1-Luc cells were seeded onto a 96-well plate (2 x 10^5 cells per well) and then treated with compounds 12 h after tetracycline addition. Cell viability and luciferase activity were determined at the same time. (Right) Cytotoxicity of compounds **18** against PANC1, DU145, and C3H10T1/2 cells. Assays were performed at 0.05 % DMSO (n=3). Error bars represent s.d.

In conclusion, chromatographic separation of the leaves of Ocimum gratissimum

Table 5-4. IC_{50} values (μM) of GLI-mediated transcriptional inhibition and cytotoxicity against cancer cells (PANC1, DU145) and C3H10T1/2 cells.

Compound	GLI transcriptional inhibition (IC_{50}, μM)	Cytotoxicity (IC_{50}, μM)		
		PANC1	DU145	C3H10T1/2
16	41.5	48.0	-	-
17	47.6	40.5	-	-
18	10.0	11.0	12.5	>40
19	103.6	108.2	-	-
20	59.4	60.0	-	-
21	57.0	58.5	-	-
22	71.5	70.6	-	-
23	70.0	69.2	-	-
24	112.8	110.5	-	-
25	120.6	120.0	-	-
26	80.0	85.5	-	-
27	105.1	112.1	-	-
28	110.3	100.7	-	-

afforded 13 known compounds. An attempt was made to examine the Hedgehog/GLI inhibition of all isolated compounds; however, only compound **18** showed moderate inhibition. The Hh/GLI signaling inhibition may be associated with the significant decrease of BCL-2 and PTCH protein level in PANC1.

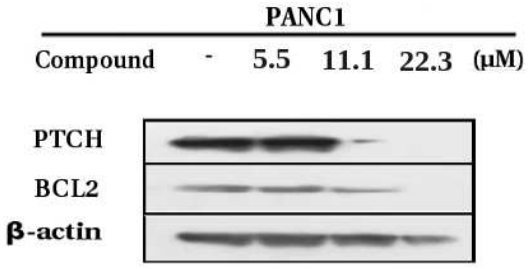

Figure 5.4: Inhibition of GLI-related protein (PTCH and BCL2) levels by compound **18** in PANC1 cells.

References

1. Ilori, M.; Sheteolu, A. O.; Omonibgehin, E. A.; Adeneye, A. A. *J. Diarrhoeal Dis Res.* **1996**, *14*, 283-285.

2. Pessoa, L. M.; Morais, S. M.; Bevilaqua, C. M. L.; Luciano, J. H. S. *Veterinary Parasitology* **2002**, *109*, 59-63.

3. Tantray, M. A.; Shawl, A. S.; Arora, B, S.; Purinama, B.; Ahmad, K.; Khuroo, M. A. *Chemistry of Natural Compounds* **2009**, *45*, 377-380.

4. Honda, C.; Suwa, K.; Takeyama, S.; Kamisako, W. *Chem. Pharm. Bull.* **2002**, *50*, 467-474.

5. Kamperdick, C.; Hong Van, N.; Sung, T. V.; Adam, G.; *Phytochemistry* **1997**, *45*, 1049-1056.

6. Fang, N.; Yu, S.; Mabry, T. J.; *Phytochemistry* **1988**, *27*, 1902-1905.

7. Yaguchi, A.; Yoshinari, T.; Tsuyuki, R.; Takahashi, H.; Nakajima, T.; Konishi, Y. S.; Nagasawa, H.; Sakuda, S. *J. Agric. Food Chem.* **2009**, *57*, 846-851.

8. Chen, C. C.; Chen, Y. P.; Hsu, H. Y.; Chen, Y. L. *Chem. Pharm. Bull.* **1984**, *32*, 166-169.

9. Le-Van, N.; Pham, T. V. C. *Phytochemistry* **1979**, *18*, 1859-1861.

10. Ayers, S.; Zink, D. L.; Mohn, K.; Powell, J. S.; Brown, C. M.; Murphy, T.; Brand, R.; Pretorius, S.; Stevenson, D.; Thompson, D.; Singh, S. B. *Phytochemistry* **2008**, *69*, 541-545.

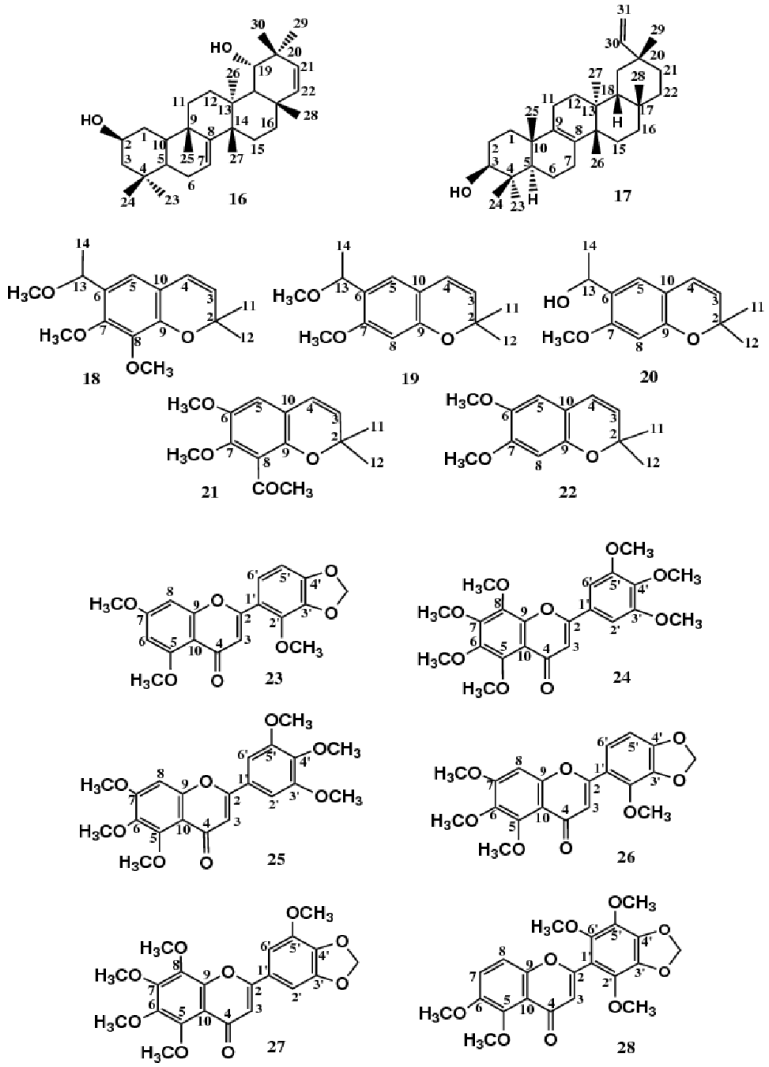

Figure 5.5: Structures of Compounds **16-28**

Table 5-1. NMR Spectroscopic data for **16-17** (in $CDCl_3$)

	Compound **16**		Compound **17**	
Position	δ_H (J in Hz)	δ_C	δ_H (J in Hz)	δ_C
1	31.6	1.13 (1H, m)	36.5	1.47 (1H, m)
2	71.2	3.49 (1H, m)	28.9	1.44 (1H, m)
3	29.0	1.21 (2H, m)	79.8	3.48 (1H, m)
4	38.3		39.7	
5	50.2	0.84 (1H, m)	50.2	0.85 (1H, m)
6	38.7	2.30 (2H, m)	19.4	2.04 (2H, m)
7	125.7	5.43 (1H, dd, 11, 5)	27.4	2.35 (2H, m)
8	140.7		134.3	
9	42.3		133.3	
10	36.5	1.53 (1H, m)	37.6	1.53 (1H, m)
11	31.8	1.22 (2H, dd, 10, 5)	21.0	1.62 (2H, dd, 8, 3)
12	34.3	1.54 (2H, dd, 10, 5)	31.8	1.51 (2H, dd, 8, 3)
13	42.2		37.3	
14	42.2		42.2	
15	29.4	1.78 (2H, dd, 10, 3.6)	25.2	1.73 (2H, dd, 9, 4)
16	37.3	1.85 (2H, d , 10)	37.3	1.87 (2H, d . 9)
17	35.6		31.6	
18	45.0	1.61 (1H, m)	44.2	1.63 (1H, m)
19	74.0	3.50 (1H, d, 3)	34.8	1.59 (1H, m)
20	31.9		34.7	
21	129.3	5.16 (1H, d, 10)	30.1	1.77 (1H, m)
22	126.4	5.18 (1H, d, 10)	35.9	1.68 (1H, m)
23	25.2	0.96 (3H, s)	28.0	0.96 (3H, s)
24	21.0	0.79 (3H, s)	16.0	0.85 (3H, s)
25	19.4	0.91 (3H, s)	19.9	0.85 (3H, s)
26	21.1	0.91 (3H, s)	24.3	1.07 (3H, s)
27	19.9	1.02 (3H, s)	20.1	1.07 (3H, s)
28	20.5	0.89 (3H, s)	31.9	1.07 (3H, s)
29	27.4	0.82 (3H, s)	154.7	5.45 (2H, dd, 10, 7)
30	24.3	0.87 (3H, s)	34.5	0.99 (3H, s)
31			107.7	5.11 (1H, d, 7)
				5.39 (1H, d, 10)

Table 5-2. NMR Spectroscopic data for **18-22** (in CD_3OD)

	Compound **18**		Compound **19**		Compound **20**	
Position	δ_H (*J* in Hz)	δ_C	δ_H (*J* in Hz)	δ_C	δ_H (*J* in Hz)	δ_C
2		76.1		76.0		72.0
3	5.45 (1H, d, 9.8)	127.8	5.47 (1H, d, 9.8)	128.2	5.48 (1H, d, 9.8)	127.8
4	6.27 (1H, d, 9.8)	122.4	6.23 (1H, d, 9.8)	121.9	6.28 (1H, d, 9.8)	121.9
5	6.95 (1H, s)	124.2	6.51 (1H, s)	129.6	6.89 (1H, s)	123.6
6		124.0		121.3		126.9
7		153.3		129.6		154.6
8		140.1	6.39 (1H, s)	100.9	6.39 (1H, s)	99.4
9		157.8		156.5		154.2
10		114.3		113.0		114.6
11	1.41 (3H, s)	28.4	1.39 (3H, s)	27.2	1.42 (3H, s)	28.0
12	1.41 (3H, s)	28.3	1.39 (3H, s)	27.0	1.42 (3H, s)	28.0
13	4.62 (1H, q, 6)	73.1	4.59 (1H, q, 6)	73.0	5.01 (1H, q, 6)	66.3
14	1.32 (3H, d, 6)	22.7	1.36 (3H, d, 6)	22.3	1.46 (3H, d, 1)	22.8
7-OCH_3	3.47 (3H, s)	51.2	3.82 (3H, s)	56.5	3.76 (3H, s)	55.3
8-OCH_3	3.21 (3H, s)	56.7				
13-OCH_3	3.75 (3H, s)	55.7	3.80 (3H, s)	55.9		

	Compound **21**		Compound **22**	
Position	δ_H (*J* in Hz)	δ_C	δ_H (*J* in Hz)	δ_C
2		76.2		75.9
3	5.51 (1H, d, 9.8)	128.7	5.46 (1H, d, 9.8)	128.2
4	6.28 (1H, d, 9.8)	122.7	6.21 (1H, d, 9.8)	121.9
5	6.63 (1H, s)	111.8	6.51 (1H, s)	109.9
6		144.3		143.1
7		151.1		149.7
8		142.1	6.39 (1H, s)	101.1
9		148.2		147.3
10		113.8		113.1
11	1.37 (3H, s)	27.9	1.39 (3H, s)	27.7
12	1.37 (3H, s)	27.7	1.39 (3H, s)	27.2
6-OCH_3	3.73 (3H, s)	56.9	3.82 (3H, s)	56.6
7-OCH_3	3.76 (3H, s)	56.0	3.81 (3H, s)	55.9
$COCH_3$		205.9		
	2.78 (3H, s)	30.0		

Table 5-3. NMR Spectroscopic data for **23-25** (in $CDCl_3$)

	Compound **23**	Compound **24**	Compound **25**	Compound **26**	Compound **27**	Compound **28**
Position	δ_H (*J* in Hz)	δ_H (*J* in Hz)	δ_H (*J* in Hz)	δ_H (*J* in Hz)	δ_H (*J* in Hz)	δ_H (*J* in Hz)
2						
3	6.57 (1H, s)	6.65 (1H, s)	6.62 (1H, s)	6.54 (1H, s)	6.58 (1H, s)	6.55 (1H, s)
4						
5						
6						
7						
8	6.77 (1H, s)		6.79 (1H, s)	6.77 (1H, s)		6.78 (1H, s)
9						
10						
1'						
2'-6'	7.04 (2H, s)	7.17 (2H, s)	7.06 (1H, s)	7.05 (2H, s)	7.09 (2H, s)	7.11 (2H, s)
3'-5'						
4'						
5-OMe	3.98 (3H, s)	3.96 (3H, s)	3.99 (3H, s)	3.97 (3H, s)	3.98 (3H, s)	3.92 (3H, s)
6-OMe		3.96 (3H, s)	3.99 (3H, s)	3.91 (3H, s)	3.98 (3H, s)	3.92 (3H, s)
7-OMe	3.95 (3H, s)	3.96 (3H, s)	3.96 (3H, s)	3.97 (3H, s)	3.95 (3H, s)	
8-OMe		3.96 (3H, s)	3.96 (3H, s)		3.95 (3H, s)	
2'-OMe	3.97 (3H, s)			3.91 (3H, s)		3.95 (3H, s)
3'-OMe		4.11 (3H, s)	3.93 (3H, s)			
4'-OMe		4.03 (3H, s)	3.93 (3H, s)			
5'-OMe		3.92 (3H, s)			4.10 (3H, s)	4.02 (3H, s)
6'-OMe						4.02 (3H, s)
O-CH_2O	6.06 (2H, s)			6.06 (2H, s)	6.09 (2H, s)	6.08 (2H, s)

Chapter 6

Separation of *Piper chaba*

Piper chaba (Piperaceae) (Figure 6.1) is a climbing glabrous creeper, cultivated in various parts of Asia, including in Bangladesh. Roots and fruits of this plant are particularly useful in asthma, bronchitis, and abdomen pain.[1] Several alkaloids containing piperidine moiety have been isolated from Piper species.[2] Lignan types were also isolated from this plant.[1]

6.1 Extraction and Isolation

MeOH extract of *Piper chaba* leaves (3.53 g) chromatographed over Diaion HP-20 to remove chlorophyll. The MeOH soluble extract (2.18 g) was then partitioned between hexane, EtOAc and BuOH. The EtOAc extract was underwent ODS open column chromatography (50 x 280 mm) to give 14 fractions. Fraction 3D (14.0 mg) was subjected to preparative HPLC [Capcell Pack C.18 type Acr, 4.6 x 250 mm; MeOH : H_2O (3 : 2); flow rate: 2.0 mL/min; RI and UV detection at 254 nm] to obtain compounds **29** (3.2 mg), **30** (1.5 mg), **31** (2.0 mg), **32** (1.7 mg), **33** (1.9 mg), and **34** (2.2 mg). Another active fraction (2G, 11.2 mg) was subjected to Sephadex LH-20 (12 x 180 mm) to get fraction 4A-4E. As fraction 4C (3.0 mg) and fraction 4D

Figure 6.1: *Piper chaba*

(3.4 mg) showed similar TLC spots, these 2 fractions were combined and subjected to preparative HPLC [Capcell Pack C.18 type Acr, 4.6 x 250 mm; MeOH : H_2O (3 :1); flow rate: 1.5 mL/min; RI and UV detection at 254 nm] to afford compounds **35** (0.8 mg), **36** (1.2 mg), **37** (0.7 mg), **38** (2.6 mg), and **39** (0.6 mg). Meanwhile, compound **40** (6.0 mg) was obtained from the separation of the active fraction 2F (8.0 mg) under preparative HPLC [Inertsil ODS-3, 10 x 250 mm; MeOH : H_2O (1 :1); flow rate: 1.5 mL/min; RI and UV detection at 254 nm].

6.2 Structure Elucidation

The continued chromatography of the EtOAc soluble fraction of *Piper chaba*, guided by Hh/GLI signaling inhibition, afforded 11 known compounds (**29**-**39**) and 1 new compound (**40**) (Figure 6.2). The basic skeleton of **29**-**40** were determined to be

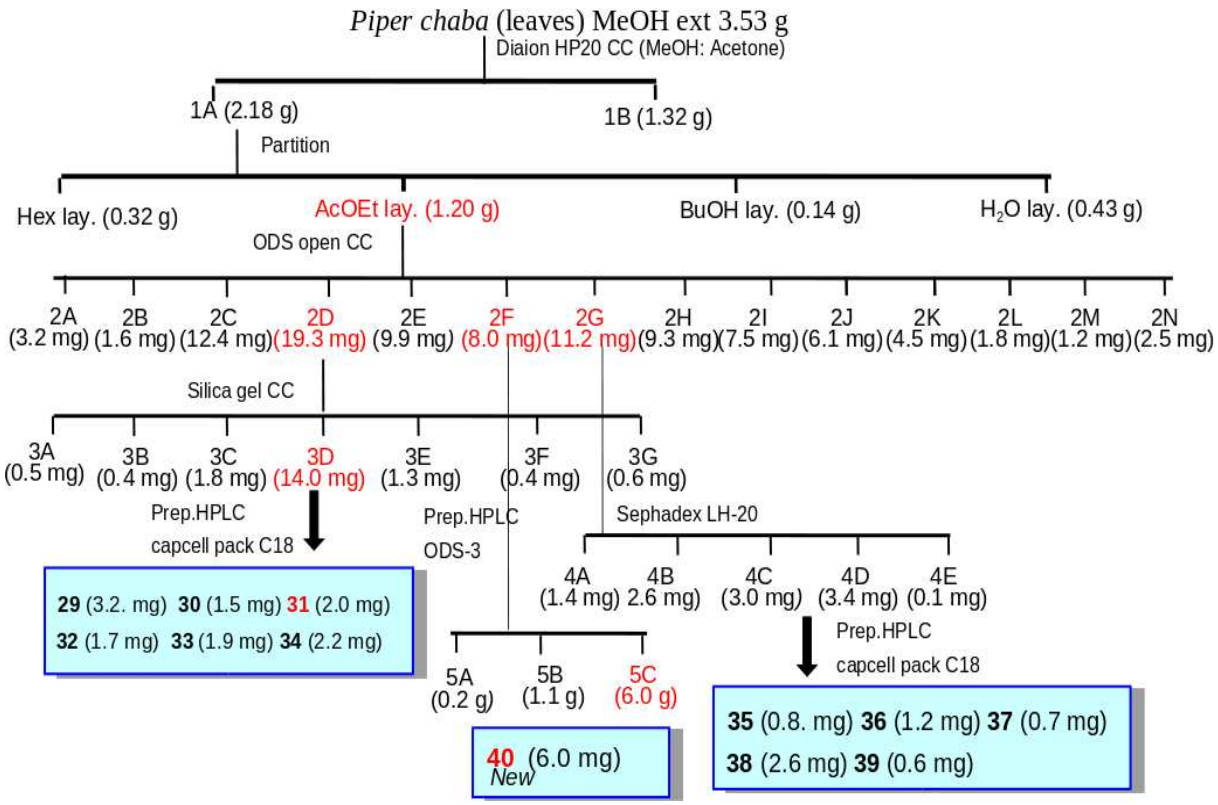

Figure 6.2: Isolation Scheme of *Piper chaba*

lignan types by virtue of a common set of ^{1}H NMR spectra that displayed 1, 3, 4 tri-substituted phenyl system possessing methylendioxy and methoxyl groups in two different ring systems.

6.2.1 Known Compounds

Kusunokinin (29)[3]

^{1}H and ^{13}C NMR data, see Table 6-3, ESIMS m/z [M + Na]$^+$ 393

3-(3,4-dimethoxy-benzyl)-4-(7-methoxy-benzo [1.3] dioxol-5-yl-methyl)-

dihydrofuran-2-one (**30**)[4]

^{1}H and ^{13}C NMR data, see Table 6-3, ESIMS *m/z* [M + Na]$^{+}$ 423

Burseran (**31**)[5]

^{1}H and ^{13}C NMR data, see Table 6-3, ESIMS *m/z* [M + Na]$^{+}$ 409

Haplomyrfolol (**32**)[6]

^{1}H and ^{13}C NMR data, see Table 6-4, ESIMS *m/z* [M + Na]$^{+}$ 381

5β-hydroxy-3",4"-dimethoxy-2-5-epoxy lignan (**33**)[7]

^{1}H and ^{13}C NMR data, see Table 6-4, ESIMS *m/z* [M + Na]$^{+}$ 395

5α-hydroxy-3",4"-dimethoxy-2-5-epoxy lignan (**34**)[7]

^{1}H and ^{13}C NMR data, see Table 6-4, ESIMS *m/z* [M + Na]$^{+}$ 395

Dihydroclusin (**35**)[8]

^{1}H and ^{13}C NMR data, see Table 6-5, FAB MS *m/z* [M + Na]$^{+}$ 427

3*R*,4*R*,5*S*-cubebin (5β-cubebin) (**36**)[9]

^{1}H and ^{13}C NMR data, see Table 6-5, FAB MS *m/z* [M + Na]$^{+}$ 379 $[\alpha]_D^{21}$ -105.0 (*c* 0.12, $CHCl_3$)

3*R*,4*R*,5*R*-cubebin (5α-cubebin) (**37**)[9]

^{1}H and ^{13}C NMR data, see Table 6-5, FAB MS *m/z* [M + Na]$^{+}$ 379 $[\alpha]_D^{21}$ -50.4 (*c* 0.07, $CHCl_3$)

Saururenin (**38**)[10]

^{1}H and ^{13}C NMR data, see Table 6-5, FAB MS *m/z* [M + Na]$^{+}$ 365

Saururin (39)[10]

^{1}H and ^{13}C NMR data, see Table 6-5 FAB MS *m/z* [M + Na]$^{+}$ 379

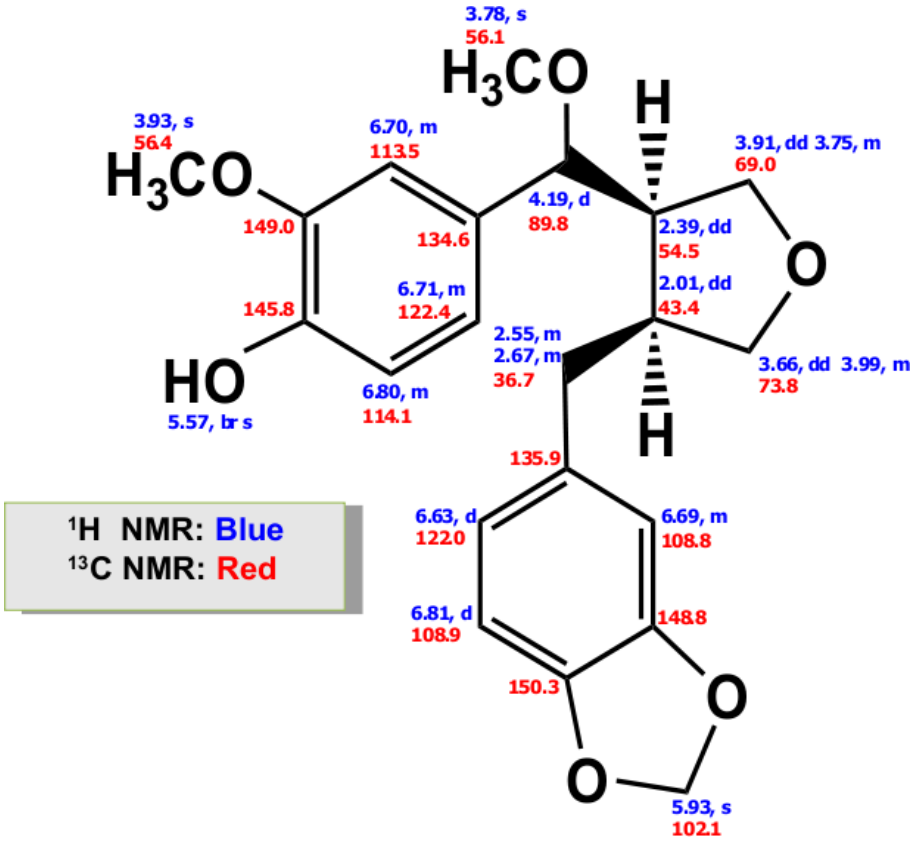

Figure 6.3: Structure of Compound **40**

6.2.2 New Compound

Compound **40** (Figure 6.3) was isolated as a white amorphous solid and gave the molecular formula $C_{21}H_{24}O_6$, as deduced from HR-FABMS *m/z* 395.1294 (calcd for $C_{21}H_{24}O_6Na$, 395.1305). The IR absorption bands suggested the presence of hydroxyl (3490 cm^{-1}) (br) and aromatic (1620, 1450 cm^{-1}) groups and methylendioxy (935 cm^{-1}). The UV absorption maxima were at UV (MeOH) λ max 282 nm (log

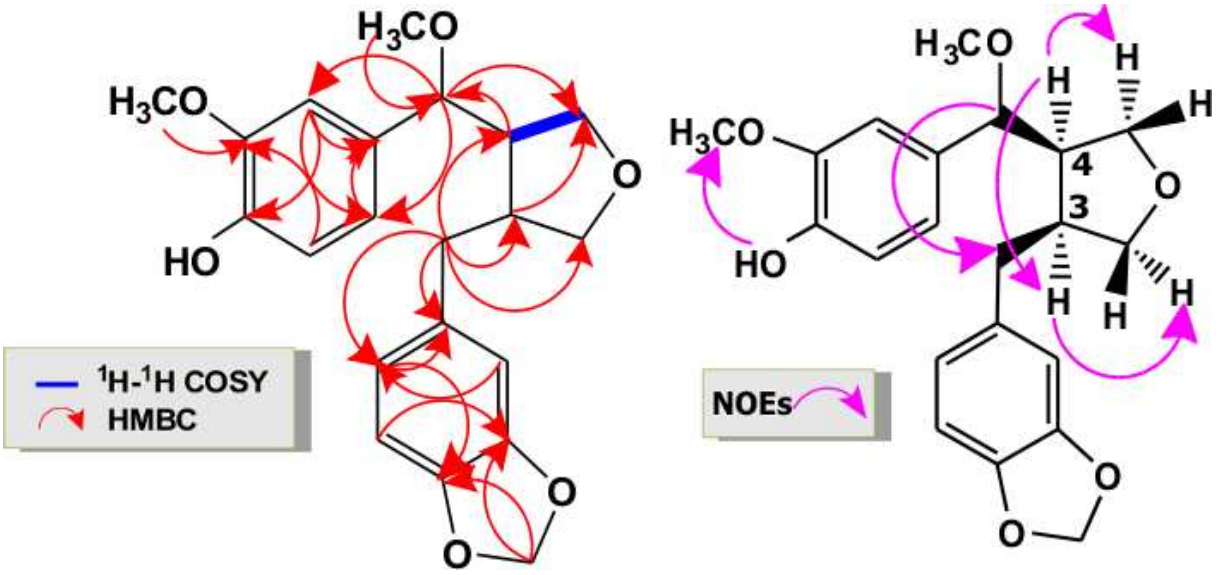

Figure 6.4: Key ^{1}H-^{1}H COSY, HMBC, and NOE correlations observed for **40**

ϵ 3.1) and 230 nm (log ϵ 3.0). The ^{1}H NMR spectrum gave a characteristic signal for the methylenedioxy function at δ 5.93. Appearance of two singlets at δ_H 3.93 and 3.78 confirmed the presence of 2 methoxyl groups. The position of these groups were confirmed by the HMBC correlation. One methoxy (δ_H 3.93) attached to C-3' (δ_C 149.0) of the benzene ring whereas another (δ_H 3.78) was attached to C-6 (δ_C 89.8) (Figure 6.4).

Although analysis of IR confirmed the presence of a hydroxyl group (3490 cm^{-1}, br), the position of -OH was difficult to assign because of the absence of HMBC signals. From NOE effects, it was found that hydroxyl protons (δ 5.57) was correlated to methoxyl proton (δ 3.78). Therefore, this data suggested that the hydroxyl group was attached at C-4'.

The stereochemistry at the chiral centres (3, 4) of **40** was assigned on the basis of both coupling constant data and NOE correlations (Figure 6.4). 1D-NOE experiments showed interaction between H-4 and H-3 as well as H-5. An NOE correlation

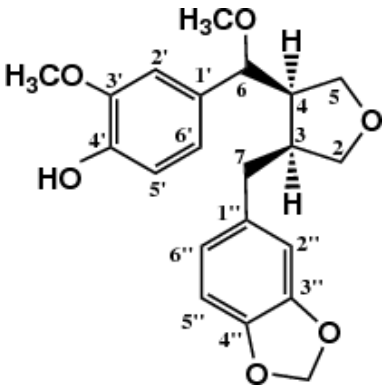

Table 6-1. ^{1}H and ^{13}C NMR spectral data of **40** (in $CDCl_3$)

Position	δ_H (J in Hz)	δ_C
1''		135.9
2''	6.69 m	108.8
3''		148.8
4''		150.3
5''	6.81 d (8.0)	108.9
6''	6.63 d (8.0)	122.0
7	2.55 m	36.7
	2.67 m	
3	2.01 dd (3.3, 13.0)	43.4
2	3.66 dd (3.3, 13.0)	73.8
	3.99 m	
1'		134.6
2'	6.70 m	113.5
3'		149.0
4'		145.8
5'	6.80 m	114.1
6'	6.71 m	122.4
6	4.19 d (3.3)	89.8
4	2.39 dd (3.3, 13.0)	54.5
5	3.75 m	72.8
	3.91 dd (3.3, 13.0)	
3'-OCH_3	3.93 s	56.4
6-OCH_3	3.78 s	56.1
OCH_2O	5.93 (2H, s)	102.1
4'-OH	5.57 br s	

was also observed between H-3 and H-2, which confirmed that both H-3 and H-4 were *cis*-oriented. These data suggested that the relative configuration (3S*, 4R*) of the chiral centres in five-membered ring of **40** was similar to that of the aforementioned compound isolated by Pu, Jian-Xin, *et al* in 2007.[11]

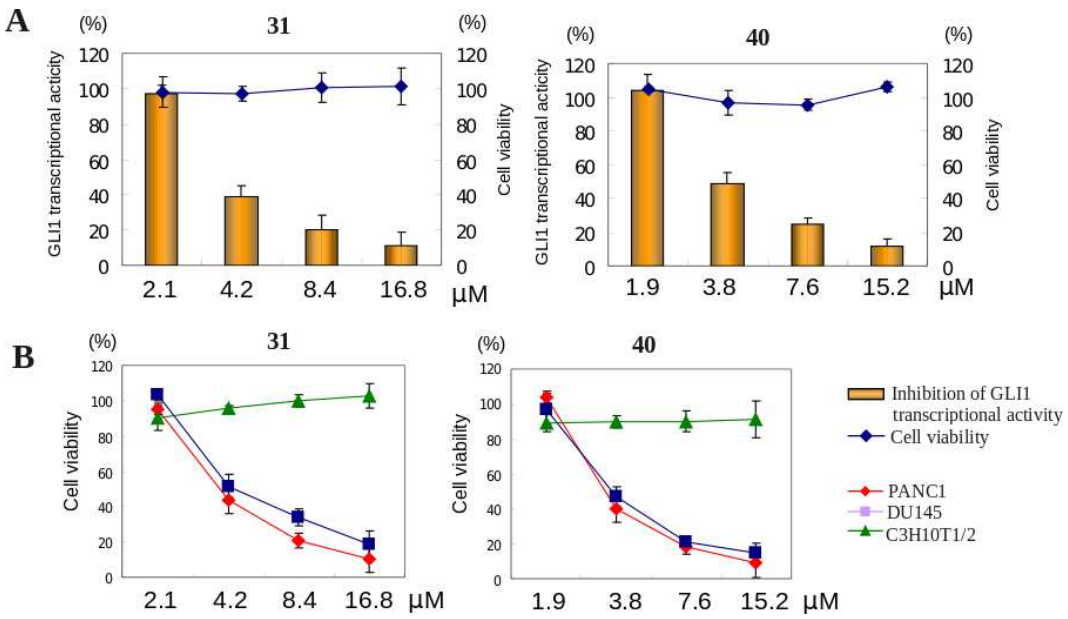

Figure 6.5: (A) Inhibition of GLI1-mediated transcriptional activity (solid columns) and cell viability (solid curves) of compounds **31** and **40**. HaCaT-GLI1-Luc cells were seeded onto a 96-well plate (2 x 10^5 cells per well) and then treated with compounds 12 h after tetracycline addition. Cell viability and luciferase activity were determined at the same time. (B) Cytotoxicity of compounds **31** and **40** against PANC1, DU145, and C3H10T1/2 cells. Assays were performed at 0.05 % DMSO (n=3). Error bars represent s.d.

6.3 Activity Assay

Hh/GLI1 inhibitory effects and cytotoxicity against cancer cells of all isolated compounds (**29-39**) were further examined. The data of IC_{50} values was summarized in Table 6-2. Among isolated compounds, **31** and **40** were apparently to be the most potent inhibitors of Hh/GLI-mediated transcriptional activity, approved by their IC_{50} values at 6.8 and 4.1 μM respectively (Figure 6.5 A, Table 6-2).

The cytotoxicity of active compounds against PANC1, DU145 and C3H10T1/2 using

Table 6-2. IC_{50} values (μM) of GLI-mediated transcriptional inhibition and cytotoxicity against cancer cells (PANC1, DU145) and C3H10T1/2 cells.

Compound	GLI transcriptional inhibition (IC_{50}, μM)	Cytotoxicity (IC_{50}, μM)		
		PANC1	DU145	C3H10T1/2
29	35.0	42.3	-	-
30	15.9	16.4	-	-
31	6.8	5.5	4.7	>30
32	17.0	18.2	-	-
33	49.6	40.0	-	-
34	18.4	21.8	-	-
35	59.8	51.0	-	-
36	75.4	72.4	-	-
37	80.0	91.6	-	-
38	42.0	35.8	-	-
39	84.5	82.5	-	-
40	4.1	4.0	5.3	>30

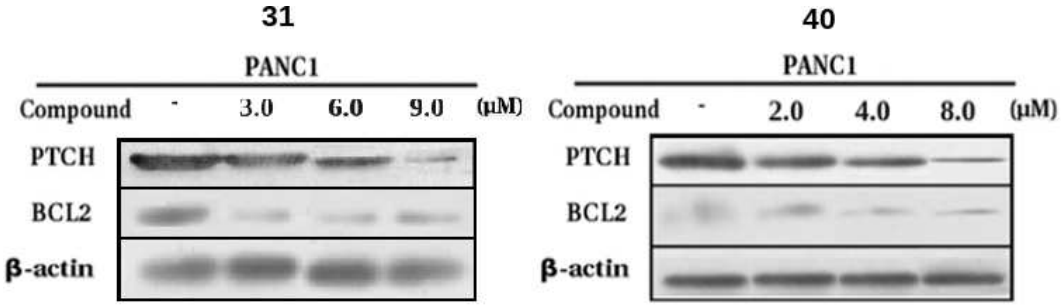

Figure 6.6: Inhibition of GLI-related protein (PTCH and BCL2) levels by compound **31** and **40** in PANC1 cells.

the FMCA system was further checked. The results revealed that compounds **31** and **40** were cytotoxic against PANC1 cells (IC_{50} values of 5.5 and 4.0 μM, respectively) and DU145 cells (IC_{50} values of 4.7 and 5.3 μM, respectively) but less affect normal cell lines (Figure 6.5 B, Table 6-2). The Western blot result further confirmed that treatment of **31** and **40** at a concentration-dependent manner led to a significant decrease in the protein level of PTCH and BCL-2 in PANC1 (Figure 6.6).

In conclusion, twelve lignan type compounds were obtained from the separation of *Piper chaba* leaves guided by Hh/GLI signaling inhibition. Compounds **31** and **40** showed strong inhibition of Hh/GLI and selected cytotoxicity against cancer cells

(PANC1, DU145). In accordance with this result, Western blot analysis confirmed that compound **31** and **40** significantly reduced the expression of tumor supressor PTCH and anti apoptosis BCL-2 in PANC1 in a dose-dependent manner.

References

1. Patra, A.; Gosh, A. *Phytochemistry* **1974**, *13*, 2889-2890.

2. Chatterjee, A.; Dutta, C. P. *Tetrahedron* **1967**, *23*, 1769-1781.

3. Sheriha, G. M.; Abouamer, K.; Elshtaiwi, B. Z.; Ashour, A. S.; Abed, F. A.; Alhallaq, H. H. *Phytochemistry* **1987**, *26*, 3339-3341.

4. Singh, M.; Tiwari, N.; Shanker, K.; Verma, R. K.; Gupta, A. K.; Gupta, M. M. *Journal of Asian Naural Products Research* **2009**, *11*, 562-568.

5. Tomioka, K.; Ishiguro, T.; Koga, K. *Chem. Pharm. Bull.* **1985**, *33*, 4333-4337.

6. Gozler, B.; Rentsch, D.; Gozler, T.; Unver, N.; Hesse, M. *Phytochemistry* **1996**, *42*, 695-699.

7. Bhandari, S. P. S.; Babu, U. V.; Garg, H. S. *Phytochemistry* **1998**, *47*, 1435-1436.

8. Prabhu, B. R.; Mulchandani, N. B. *Phytochemistry* **1985**, *24*, 329-331.

9. de Pascoli, I. C.; Nascimento, I. R.; Lopes, L. M. X. *Phytochemistry* **2006**, *67*, 735-742.

10. Rao, K, V.; Rao, N. S. P. *J. Nat. Prod.* **1990**, *53*, 212-215.

11. Pu, X. J.; Xiao, W, L.; Li, H. M.; Huang, S. X.; Sung, H. D. *Helvetica Chim. Acta* **2007**, *90*, 723-729.

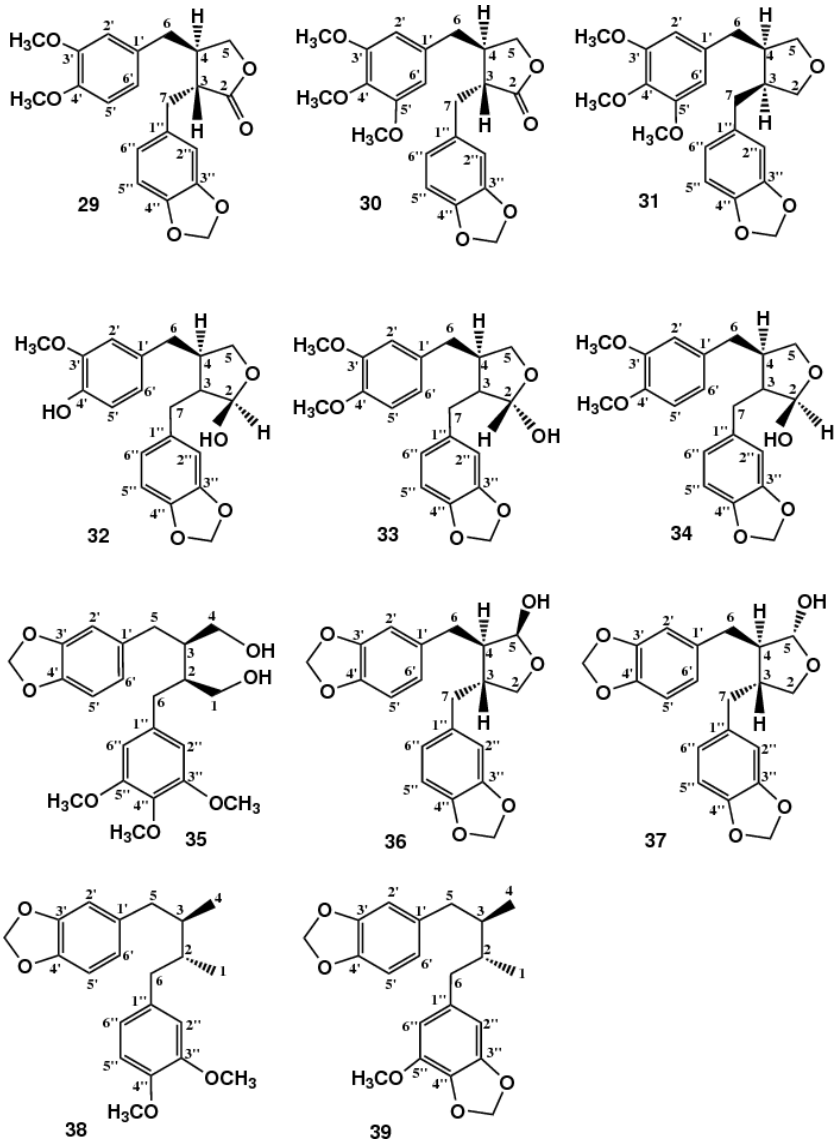

Figure 6.7: Structures of Compounds **29-39**

Table 6-3. NMR Spectroscopic data for **29-31** (in $CDCl_3$)

	Compound **29**		Compound **30**		Compound **31**	
Position	δ_H (*J* in Hz)	δ_C	δ_H (*J* in Hz)	δ_C	δ_H (*J* in Hz)	δ_C
1"		131.4		130.6		134.1
2"	6.58 d (2.0)	109.1	6.67 br s	111.8	6.67 m	108.0
3"		147.9		149.6		145.8
4"		146.5		148.5		147.6
5"	6.68 d (7.9)	108.0	6.69 d (9.0)	112.9	6.69 m	108.9
6"	6.53 dd (8.0, 1.9)	121.7	6.75 d (9.0)	121.7	6.74 m	121.4
7	2.92 dd (14.0, 7.0)	38.3	2.92 m, 2.96 m	35.4	2.70 m, 2.66 m	39.9
3	2.51 m	46.5	2.59 m	46.9	2.54 m	46.3
2		178.4		178.8	4.11 dd (8.9, 7.0)	73.2
1'		130.4		132.7	3.85 m	136.1
2'	6.46 br s	111.4	6.16 br s	102.8	6.16 br s	105.6
3'		149.1		143.9		153.1
4'		149.2		134.4		136.4
5'	6.75 d (8.0)	111.7		149.6		153.1
6'	6.54 dd (8.0, 1.9)	122.3	6.14 br s	109.4	6.14 br s	105.6
6	2.61 dd (11.0, 4.5)	34.8	2.53 , 2.44 m	39.1	2.53 , 2.44 m	39.9
4	2.56 m	41.2	2.49 m	41.6	2.49 m	46.3
5	4.15 dd (9.0, 7.1)	71.2	4.15 dd (9.0, 7.1)	71.5	4.15 dd (9.0, 7.1)	73.2
	3.98 dd (9.0, 7.6)		3.85 m		3.85 m	
3'-OCH_3	3.81 s	55.9	3.83 s	56.2	3.83 s	56.0
4'-OCH_3	3.84 s	55.7	3.81 s	56.3	3.81 s	56.0
5'-OCH_3			3.91 s	57.2	3.91 s	60.8
OCH_2-O	5.92 (2H, d, 4.2)	100.8	5.92 (2H, s)	101.7	5.92 (2H, s)	100.8

Table 6-4. NMR Spectroscopic data for **32-34** (in $CDCl_3$)

	Compound **32**		Compound **33**		Compound **34**	
Position	δ_H (*J* in Hz)	δ_C	δ_H (*J* in Hz)	δ_C	δ_H (*J* in Hz)	δ_C
1"		133.3		134.5		133.3
2"	6.54 d (1.5)	109.1	6.45 d (2.0)	109.1	6.45 d (2.0)	109.3
3"		147.6		147.2		147.5
4"		145.8		145.5		145.7
5"	6.67 d (7.6)	107.9	6.78 d (8.0)	108.1	6.76 d (8.0)	108.1
6"	6.53 dd (8.5, 2.0)	121.7	6.52 dd (8.0, 1.8)	121.6	6.53 dd (8.0, 1.8)	121.7
7	2.42 m, 2.63 m	38.4	2.68 m, 2.82 m	39.1	2.61 m, 2.73 m	38.7
3	2.15 m	53.1	2.15 m	45.9	1.98 m	42.8
2	5.21 d (1.6)	103.4	5.21 m	103.6	5.21 m	98.8
1'		132.2		132.7		132.9
2'	6.51 d (2.0)	111.1	6.47 br s	111.7	6.47 br s	111.8
3'		146.3		148.7		148.8
4'		143.8		147.3		147.7
5'	6.76 d (8.0)	114.3	6.70 d (7.5)	111.2	6.74 d (7.5)	111.3
6'	6.56 dd (8.0, 2.0)	121.2	6.49 dd (7.5, 1.5)	120.9	6.49 dd (7.5, 1.5)	120.5
6	2.59 m, 2.61 m	39.2	2.57 m, 2.75 m	39.1	2.57 m, 2.73 m	33.6
4	2.16 m	45.9	2.20 m	53.1	2.43 m	52.1
5	3.81 t (8.0)	72.2	3.97 dd (7.0, 8.0)	72.2	4.09 t (8.0)	72.6
	4.08 dd (8.0, 7.0)		3.84 m		3.99 t (8.0)	
3'-OCH_3	3.85 s	55.8	3.83 s	55.8	3.81 s	55.8
4'-OCH_3			3.81 s	55.7	3.83 s	55.7
OCH_2-O	5.91 (2H, s)	100.8	5.92 (2H, s)	100.8	5.90 (2H, s)	100.8

Table 6-5. NMR Spectroscopic data for **35-39** (in $CDCl_3$)

	Compound **35**	Compound **36**	Compound **37**	Compound **38**	Compound **39**
Position	δ_H (J in Hz)	δ_H(J in Hz)	δ_H (J in Hz)	δ_H(J in Hz)	δ_H(J in Hz)
1"					
2"	6.40 s	6.67 d (2.0)	6.56 d (2.0)	6.79 m	6.72 m
3"					
4"					
5"		6.66 d (8.0)	6.67 d (8.0)	6.79 m	
6"	6.40 s	6.66 d (8.0)	6.49 d (8.0, 2.0)	6.79 m	6.72 m
7	2.69 m	2.48 m 2.70 dd (14.0, 8.0)	2.60 m, 2.61 m	2.42 m	2.40 m
3	1.87 m	2.30 m	2.08 m	1.34 s	1.29 s
2	3.43 m	3.47 dd (8.0, 7.0) 4.07 t (8.0)	3.72 dd (8.0, 9.0) 3.94 dd (8.0, 7.0)	0.81 d (7.0)	0.88 d (7.0)
1'					
2'	6.64 s	6.50 d (2.0)	6.45 d (2.0)	6.79 m	6.72 m
3'					
4'					
5'	6.72 d (8.2)	6.66 d (8.0)	6.66 d (8.0)	6.79 m	6.72 m
6'	6.52 d (8.2)	6.52 dd (8.0, 2.0)	6.44 dd (8.0, 2.0)	6.79 m	6.72 m
6	2.69 m	2.37 m, 2.59 m	2.32 m, 2.61 m	2.42 m	2.42 m
4	1.87 m	1.93 m	2.08 m	1.34 s	1.34 s
5	3.72 m	5.15 d (4.0)	5.15 d (1.5)	0.81 d (7.0)	0.88 d (7.0)
5-OH		2.70 br s	1.70 br s		
3"-OCH_3	3.81 s			3.78 s	3.82 s
4"-OCH_3	3.83 s			3.78 s	
5"-OCH3	3.83 s				
OCH_2-O	5.92 (2H, s)	5.93 (4H, s)	5.93 (4H, s)	5.91 (2H, s)	5.93 (4H, s)

Chapter 7

Experimental

7.1 General

Optical rotation	:	JASCO P-1020 polarimeter
UV spectra	:	Shimazu UV mini-1240 spectrometer
CD spectra	:	JASCO J-720W1 spectrometer
IR spectra (ATR)	:	JASCO FT-IR 230 spectrometer
NMR spectra	:	JEOL A 400, JEOL A 500, ECP 400, ECP 600 spectrometers (deuterated solvents, the chemical shift of which was used as an internal standard)
FABMS	:	JEOL JMS-AX500 spectrometer
HRFABMS	:	JEOL HX-110A spectrometer
HREIMS	:	JEOL JMS-AX500 spectrometer
HRESIMS	:	Thermo scientific exative
Incubator	:	CO_2 MCO-17A$_1$, SANYO 37^0C 5% CO_2
Clean beanch	:	Bio Clean Bench MCV-B131S, SANYO
RT PCR	:	Termal Cycler Dice (TaKaRa) Mx3000P QPCR system (Stratagene)

Cell Culture

HaCaT Human keratinocyte-GLI1
HaCaT-GLI1 (gifted by Dr. Fritz Aberger and Gerhard Regl)
Dulbecco's modified Eagle Medium (DMEM, high glucose, Wako) + 5% fetal bovine serum (FBS, biowest)

HaCaT-GLI1-luc
DMEM (high glucose, Wako) + 5 % FBS and Penicillin (200 unit/mL) or Streptomycin (200 mg/mL) (Gibco)

PANC1 (human pancreatic cancer cell, provided by RIKEN BRC)
RPMI-1640 (Wako) + 10 % FBS

DU145 (human prostate cancer cell, provided from Cell Resource Center for Biomedical Research Institute of Development, Aging and Cancer Tohoku University)
RPMI-1640 (Wako) + 10%FBS

C3H10T1/2 (mouse embryonic fibroblast cell, provided by RIKEN BRC)
DMEM (high glucose, Wako) + 10 % FBS

Fetal Bovine Serumn (FBS, Biowest), Trypsin EDTA (0.25% Trypsin-EDTA, Gibco)Trypan blue (0.4%(w/v) trypan blue, Nacalai tesque Inc.), Penicillin (10,000 unit/mL) Streptomycin (10,000 g/mL) (Gibco), Blasticidin S Hcl (Invitrogen), Zocin (Invitrogen), Puromycin (SIGMA), Tetracycline (Invitrogen).

PBS :

KCl (Nacalai tsque Inc.)	0.2 g
KH2PO4 (Nacalai tesque Inc.)	0.2 g
NaCl (Nacalai tesque Inc.)	8.0 g
Na_2HPO_4 (Nacalai tesque Inc.)	1.11 g
dH_2O	up to 1 L (autoclaved; 121^0C, 20 min)

SDS-PAGE

	Running gel			Stacking gel
Material	12.5%	10 %	7.5 %	5 %
H_2O	2.2 mL	3.1 mL	3.9 mL	3.4 mL
30 % acrylamide	4.2 mL	3.3 mL	2.5 mL	0.83 mL
1 M Tris-HCl (pH 8.8)	3.4 mL	3.4 mL	3.4 mL	—
1 M Tris-HCl (pH 6.8)	—	—	—	0.63 mL
10 % SDS	0.1 mL	0.1 mL	0.1 mL	0.05 mL
10 % ammonium persulfate	0.1 mL	0.1 mL	0.1 mL	0.05 mL
TEMED	7 μL	7 μL	7 μL	3 μL

10 x Running Buffer:

Tris	30.3 g (0.25 M)
glycin	144 g (1.92 M)
SDS	10 g (1 % (w/v))
dH_2O	up to 1 L

5 x SDS Buffer:

0.5 M Tris-HCl (pH 6.8)	15.7 mL (0.313 M)
SDS	2.5 g (10 % (w/v))
sucrose	6.25 g (25 %(w/v))
bromo phenol blue	6.25 mg (0.025 % (w/v))
dH_2O	up to 25 mL

TBST (Tris-Buffered Saline Tween 20):

Tris	3.6 g
NaCl	17.4 g
conc.HCl	2.4 mL
Tween 20	3.0 g
dH_2O	up to 3 L

Lysis Buffer:

1 M Tris-HCl	2 mL (20 mM)
NaCl	878 mg (150 mM)
Triton X-100	0.5 mL (0.5% (w/v))
sodium deoxycholate	500 mg (0.5 % (w/v))
EDTA	292.2 mg (10 mM)
sodium orthovanadate (Na_3VO_4)	18.4 mg (1 mM)
sodium fluoride (NaF)	0.42 mg (0.1 mM)
protease inhibitor cocktail	1 mL (1 %(v/v))
dH_2O	up to 100 mL

30 % Acrylamide:

Acrylamide	29.2 g
N, N'-methylene-bis-acrylamide	0.8 g
dH_2O	up to 100 mL

7.2 Plant Material

7.2.1 Medicinal Plants Collected from Thailand

The leaves of *Acacia pennata* and *Vallaris glabra* were collected in Thailand and they were sent to Japan on 26th February 2008. Plants were identified by Dr. Thaworn Kowithayakorn, and voucher specimens (KKP0023 and KKP0252) have

been deposited in both Khon Kaen University (Thailand) and the Graduate School of Pharmaceutical Sciences, Chiba University (Japan).

7.2.2 Medicinal Plants Collected from Bangladesh

The leaves of *Excoecaria agallocha*, *Ocimum gratissimum*, and *Piper chaba* were collected in Bangladesh in November 2008. Plants were taxonomically identified by Prof. A. K. Fazlul Huq, Forestry and Wood Technology Discipline, Khulna University, Bangladesh, and voucher specimens (KKB034, KKB054, and KKB108) have been deposited there for future reference.

7.3 Western Blotting

7.3.1 Isolation of Cellular Extracts

PANC1 cells were seeded into 10 cm dishes (2 x 10^6 cells) and incubated for 24 h at 37^0C. Compounds at various concentrations were added. After 24 h incubation, cells were washed with PBS and then collected by scraping the whole parts. Protein lysate was prepared with lysis buffer (20 mM Tris-HCl pH 7.4, 150 mM NaCl, 0.5 % sodium deoxycholate, 10 mM EDTA, 1 mM sodium orthovanadate, and 0.1 mM NaF) containing a 1 % proteasome inhibitor cocktail (Nacalai Tesque, Japan), and then centrifuged at 13000 rpm, 4^0C for 30 min.

7.3.2 Isolation of Cytosolic and Nuclear Proteins

PANC1 cells were seeded into 60 mm dishes (2 x 10^6 cells), and incubated for 24 h at 37^0C, after which cells were harvested with trypsin and centrifuged at 1000 rpm at

4^0C for 5 min. Protein lysates were prepared in the same way as the isolation of the whole cellular extract. Nuclear and cytosolic extracts were prepared using NE-PER nuclear and cytosolic extraction reagents (Pierce) according to the manufacturer's instructions.

7.3.3 Western Blotting Procedure

HaCaT-expressed exogenous GLI1 cells were seeded onto a 10 cm dish (2 x 10^6 cells/ dish), and incubated for 12 h at 37^0C. To activate expression of exogenous GLI1 protein, 1 g/mL of tetracycline was added into each well, followed by another 12 h incubation. DMEM medium (containing 5% FBS) was removed and compounds at various concentrations were added.

After 24 h incubation, cells were washed with PBS then homogenized in lysis buffer (20 mM Tris-HCl pH 7.4, 150 mM NaCl, 0.5% sodium deoxycholate, 10 mM EDTA, 1 mM sodium orthovanadate, and 0.1 mM NaF) containing 1% proteasome inhibitor cocktail (Nacalai Tesque, Tokyo, Japan), and incubated on ice for 30 min. Supernatants of the cell lysates, as obtained from a 4^0C centrifugation (30 min), were subjected to a 5% and 12.5% SDS-PAGE electrophoresis then transferred to a polyvinylidine difluoride (PVDF) membrane (Bio-Rad).

Blots were blocked with TBST (10 mM Tris-HCl pH 7.4, 100 mM NaCl and 0.1% Tween 20) containing 5% skimmed milk for 1 h and hybridized at room temperature for 1 h with primary antibodies: GLI1, PTCH (Santa Cruz) and BCL-2 (Sigma). Another 1 hr incubation of blots-hybridized secondary antibodies was performed at room temperature. The secondary antibodies used were anti-goat IgG (Sigma), anti-rabbit IgG, and anti-mouse IgG (Amersham Biosciences). After washing with TBST, immunocomplexed bands were detected using an ECL Advance Western (GE Healthcare Biosciences) or an Immobilon Western (Millipore) detection system.

To confirm protein expression level of PTCH and BCL-2 in PANC1, the same method as described above was performed. PANC1 cells were seeded onto a 6 cm dish (1 x 10^6 cells/ dish), and incubated for 12 h at 37^0C. Compounds, dissolved in DMSO, replaced RPMI-1640 medium (containing 10 % FBS) after 24-h incubation. Homogenization and addition of lysis buffer were performed after 24 h to obtain whole protein lysates. Furthermore, protein lysates of the whole extract, cytosol or nucleus were blotted and blocked using similar procedures.

To detect GLI1 (150 kDa), PTCH (140 kDa) and BCL-2 (26 kDa), anti-GLI1 (Santa Cruz Biotechnology), anti PTCH (Santa Cruz Biotechnology), and anti BCL-2 (Sigma) were used as specific primary antibodies followed by anti-goat IgG (Sigma), anti-rabbit IgG, and anti-mouse IgG (Amersham Biosciences) as the second antibodies. β-actin (45 kDa) was used as an internal control.

7.4 RNA Interference Experiments

PANC1 cells were seeded into 6 cm dishes (4 x 10^5 cells) and incubated for 12 h. RPMI-1640 medium (containing 10 % FBS) was removed and compounds at different concentration were added. After 12 h incubation, cells were transfected with small interfering RNA (20 nM) (SMO siRNAs, Santa Cruz Biotechnology) using SiPORTTM NeoFXTM (Ambion) and OPTI-MEM (Invitrogen), as described by the manufacturer. Transfection of a non-targeting siRNA at the same concentration served as a control (the compound was replaced by DMSO).

To confirm the transfection efficiency of RNA interference, Western blotting was performed prior to quantitative RT-PCR. Anti Smo (Santa Cruz Biotechnology) and anti-rabbit IgG (Jackson ImmunoResearch Lab. Inc.) were used as first and secondary antibodies, respectively, followed by enhanced chemiluminescence detection (GE Healthcare Biosciences).

7.5 Real Time Polymerase Chain Reaction

7.5.1 Reaction Condition

Reverse transcription:

Incubation	25^0C	10 min
Reverse transcription reaction	42^0C	50 min
Deactivation of enzyme	95^0C	15 sec

RNA degradation:

RNA degradation	37^0C	20 min

Primers:

GLI1;	forward	5'-GCCGTGTAAAGCTCCAGTGAACACA-3'
	reverse	5'-TCCCACTTTGAGAGGCCCATAGCAAG-3' (200 bp product)
Ptch;	forward	5'-TCCTCGTGTGCGCTGTCTTCCTTC-3'
	reverse	5'-CGTCAGAAAGGCCAAAGCAACGTGA-3' (200 bp product)
Bcl2;	forward	5'-TGGACAACCATGACCTTGGACAATCA-3'
	reverse	5'-TCCATCCTCCACCAGTGTTCCCATC-3'
Gapdh;	forward	5'-ATGGGGAAGGTGAAGGTCG-3'
	reverse	5'-TAAAAGCAGCCCTGGTGACC-3'

PCR condition:

Initial incubation	50^0C	2 min
Initial denaturation	95^0C	2 min
Denaturation	95^0C	15 sec. 40 cycles
Annealing, extension	60^0C	30 sec.
Dissociation curve analysis	60^0C	30 sec. 95^0C 30 sec.

7.5.2 RT-PCR Procedure

Total RNA was extracted using an Rneasy Mini kit (Qiagen), and cDNA was synthesized using the RT-PCR SuperScript III Platinum Two Step qRT-PCR Kit (Invitrogen). The mRNA levels of Ptch were measured on a Mx3000P QPCR system (Stratagene) at the following annealing temperatures: 50^0C for 2 min (initial incubation), 95^0C for 2 min (initial denaturation), and then 40 cycles of 95^0C for 15 s (denaturation) and 60^0C for 30 s (annealing, extension). Each amplification reaction was performed in triplicate. mRNA quantification is expressed in arbitrary units and was normalized to an internal control GAPDH.

Appendix I

Screening of Bangladesh Plant Extracts

KKB001-KKB035

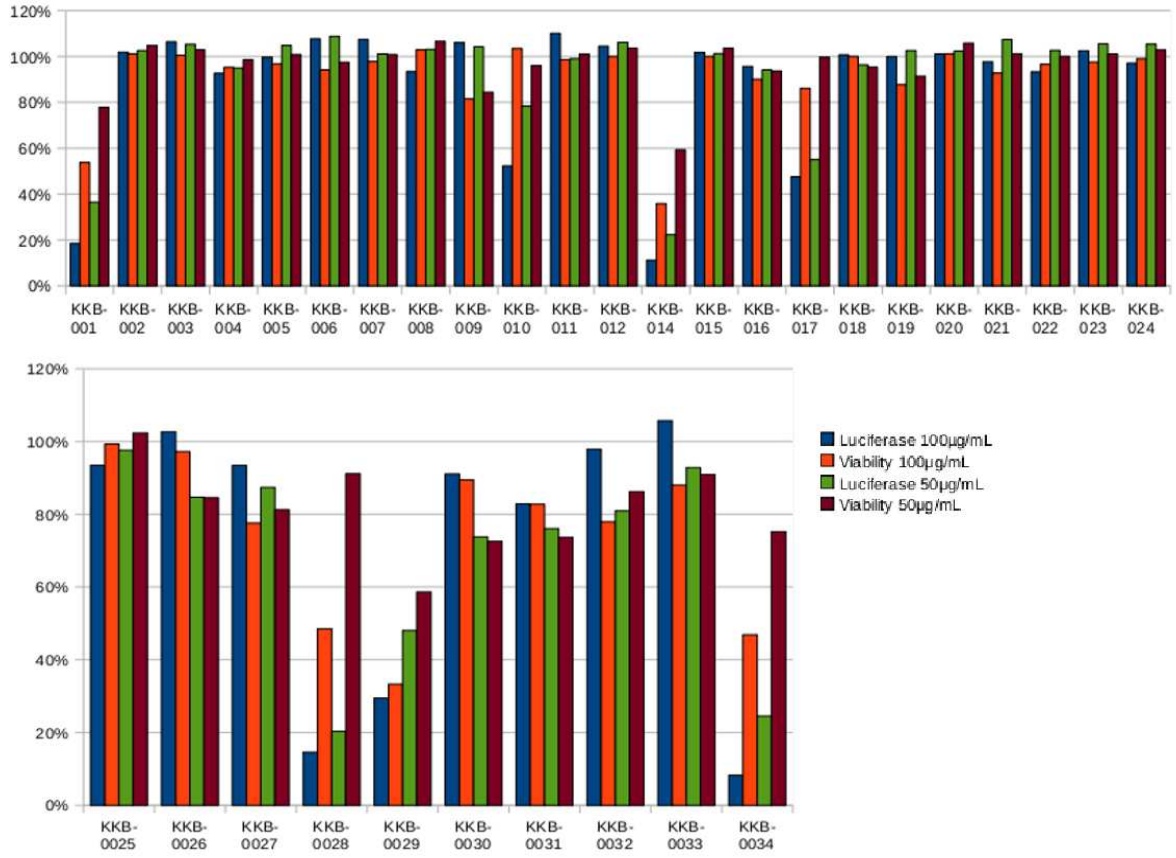

KKB035-KKB056

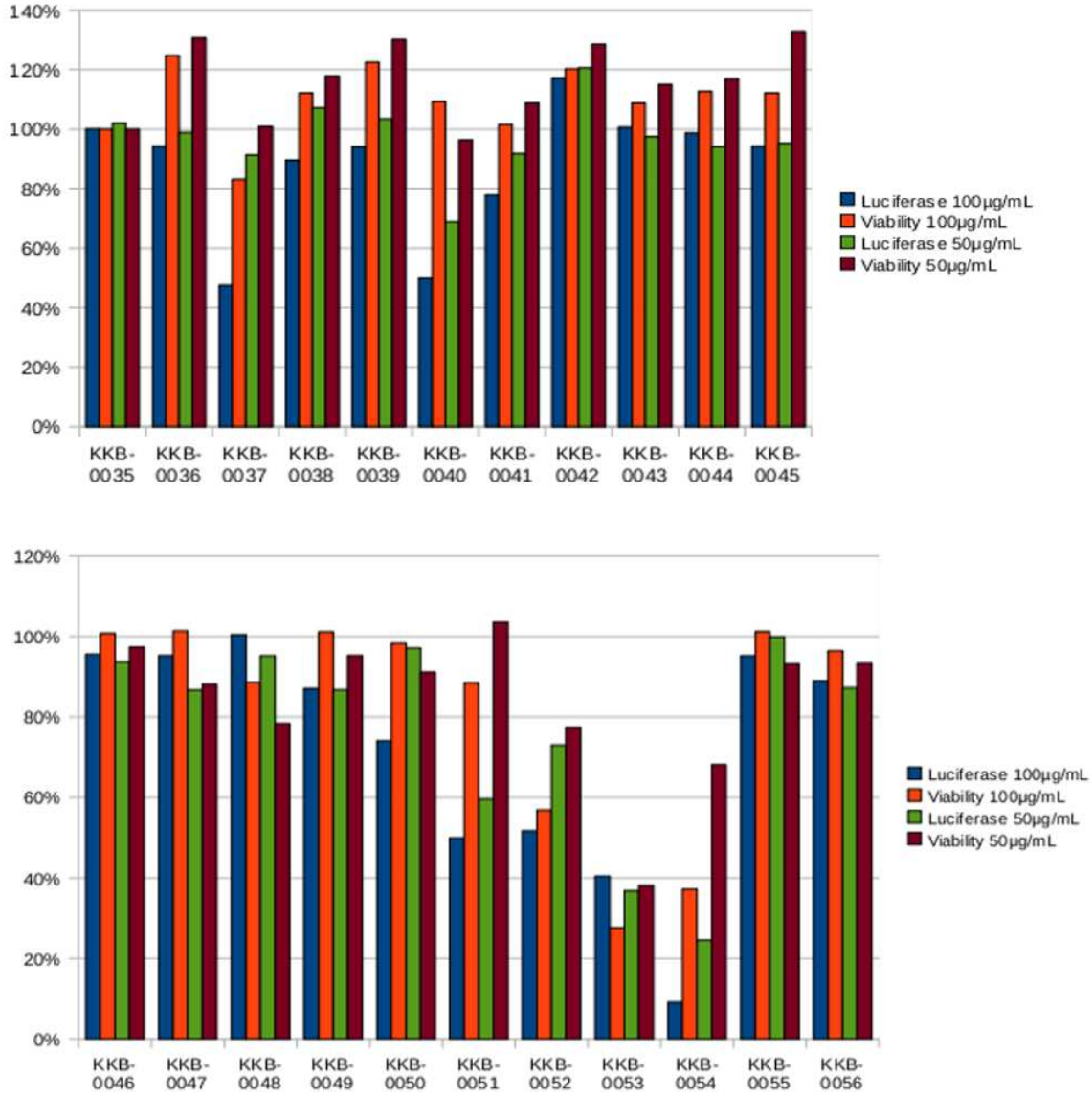

KKB101-KKB117

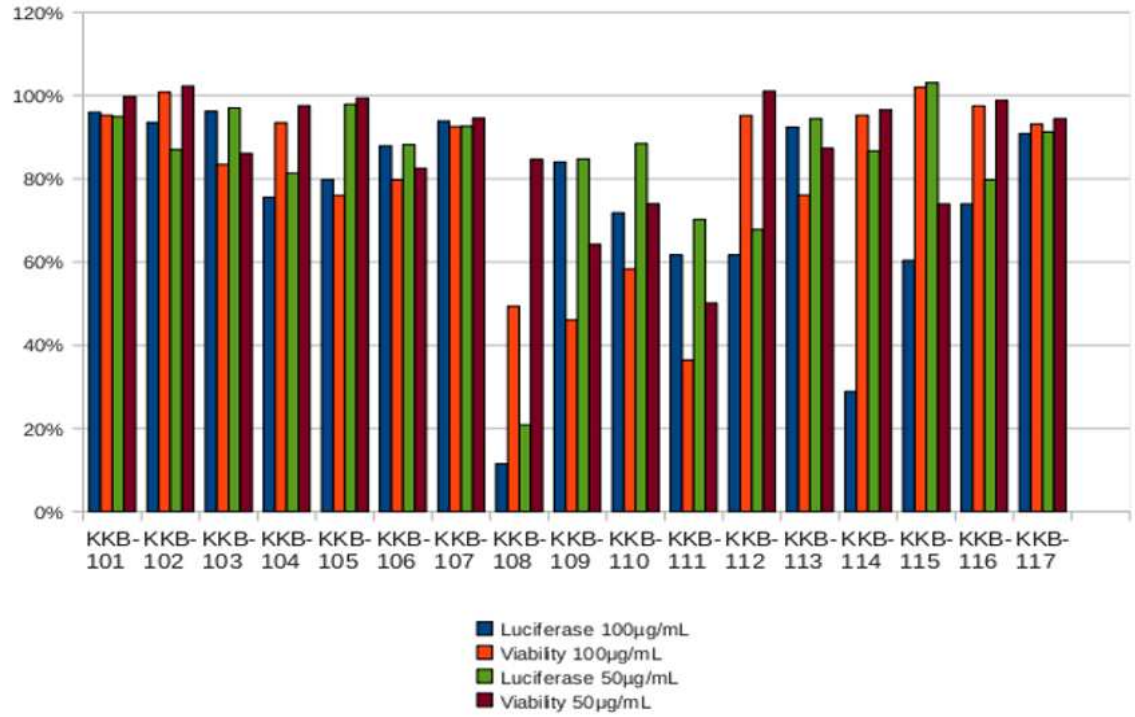

Appendix II

List of Bangladesh Plant Extracts

KKB001	*Adiantum philipense* (Leaves)
KKB002	*Asparagus racemosus* (Roots)
KKB003	*Centella asiatica* (Whole plant)
KKB004	*Commelina benghalensis* (Roots)
KKB005	*Flemingia congesta* (Leaves)
KKB006	*Hygrophila spinosa* (Seed)
KKB007	*Mesua ferrea / M. nagassarium* (Flower)
KKB008	*Ocimum sanctum* (Whole plant)
KKB009	*Sida acuta* (Whole plant)
KKB010	*Sida rhombifolio* (Whole plant)
KKB011	*Vitex negundo* (Leaves)
KKB012	*Derris indica* (Leaves)
KKB013	*Derris trifoliata* (Aerial part)
KKB014	*Physalis minima*
KKB015	*Excoecaria indica* (Leaves)
KKB016	*Terminalia bellerica*
KKB017	*Ficus racemosus* (Fruits)
KKB018	*Ipomoea maxina*

KKB019 *Cleoma rutidosperma*

KKB020 *Cricus arvensis*

KKB021 *Acacia spp.*

KKB022 *Heritiera fomes* (Leaves)

KKB023 *Xylocarpus granatum* (Leaves)

KKB024 *Hibiscus tiliaceus* (Leaves)

KKB025 *Ceriops decandra* (Leaves)

KKB026 *Rhizopora spp.* (Leaves)

KKB027 *Sonneratia caseolaris* (Leaves)

KKB028 *Veronia spp.* (Stem)

KKB0029 *Lumnitzera racemosus* (Leaves)

KKB0030 *Acanthus ilicifolius* (Aerial part)

KKB0031 *Crataeva nurvala* (Aerial part)

KKB0032 *Clerodendrum inerme* (Leaves)

KKB0033 *Cerbera manghas* (Leaves)

KKB0034 *Exocoecaria agallocha* (Leaves)

KKB0035 *Avicennia marina* (Leaves)

KKB0036 *Ocimum gratissimum* (Aerial part)

KKB0037 *Thevetia peruviana* (Aerial part)

KKB0038 *Rhizophoria epiculata* (Leaves)

KKB0039 *Amoora cucullata* (Leaves)

KKB0040 *Rhizophora mucronata* (Leaves)

KKB0041 *Derris trifoliate* (Aerial part)

KKB0042 *Rhizophora mucronata* (Leaves)

KKB0043 *Acrostichum aurium* (Aerial part)

KKB0044 *Cocculus villosus* (Leaves with small stem)

KKB0045 *Kandelia candela* (Leaves)

KKB0046 *Aegiceras corniculatum* (Leaves)

KKB0047 *Renhydra sp.* (Aerial part)

KKB0048 *Curcuma zedoaria* (Aerial part)

KKB0049 *Mallotus spp.* (Leaves with small stem)

KKB0050 *Urginea indica* (Aerial part)

KKB0051 *Alombus spp.* (Aerial part)

KKB0052 *Pongamia pinnata* (Leaves)

KKB0053 *Pongamia pinnata* (Fruits)

KKB0054 *Ocimum gratissimum* (Leaves)

KKB0055 *Cyperus spp.* (Whole plant)

KKB0056 *Pandanus foetidus* (Aerial part)

KKB0101 *Murraya koenigii* (Leaves)

KKB0102 *Swietenia mahagoni* (Leaves)

KKB0103 *Aegle marmelos* (Leaves)

KKB0104 *Seseli diffusum* (Seeds)

KKB0105 *Alostonia scholaris* (Stem Barks)

KKB0106 *Vallaris solanacea* (Leaves)

KKB0107 *Vallaris solanacea* (Stem)

KKB0108 *Piper chaba* (Leaves)

KKB0109 *Piper chaba* (Roots)

KKB0110 *Primna integrifolia* (Leaves and stems)

KKB0111 *Phyllanthus emblica* (Fruits)

KKB0112 *Terminalia bellirica* (Fruits)

KKB0113 *Terminalia chebula* (Fruits)

KKB0114 *Boerhavia diffusa* (Leaves and stems)

KKB0115 *Ruellia tuberosa* (Stem)

KKB0116 *Saussurea hypoleucav* (Roots)

KKB0117 *Solanum indicum* (Leaves and stems)

Appendix III

Characteristics of New Compounds

Compound **6**: Yellow powder, $[\alpha]_D^{20}$ -140 (c 0.1, MeOH), UV(MeOH) λ max (log ϵ) 261 nm (3.8); 355 nm (3.0); IR (ATR) max 3317 (br), 2948, 2835, 1652, 1449, 1417, 1015 cm^{-1}; HR-FABMS m/z 485.1162 $[M+Na]^+$ (calcd for $C_{22}H_{24}O_{11}Na$, 485.1173) ; ^1H NMR and ^{13}C NMR (DMSO-d_6) (Table 3-1).

Compound **7**: Yellow amorphous solid, $[\alpha]_D^{20}$ -152 (c 0.3, MeOH), UV(MeOH) λ max (log ϵ) 259 nm (3.1); 362 nm (2.5); IR (ATR) max 3333 (br), 2944, 2832, 1655, 1449, 1364, 1117 cm^{-1} ; HRESIMS m/z 617.1584 $[M+Na]^+$ (calcd for $C_{27}H_{30}O_{15}Na$, 617.1558) ; ^1H NMR and ^{13}C NMR (DMSO-d_6) (Table 3-1).

Compound **14**: Pale yellow powder; $[\alpha]_D^{20}$ -32 (c 0.11, MeOH); UV (MeOH) λ max (log ϵ) 216 nm (3.8) and 275 nm (2.1); IR (ATR) max 3395 (br), 2922, 1733, 1568, and 1447 cm^{-1}; HR-FABMS m/z 657.3353 $[M+Na]^+$ (calcd for $C_{34}H_{50}O_{11}Na$, 657.3366); ^1H NMR and ^{13}C NMR (Pyridine-d_5) (Table 4-2).

Compound **40**: White amorphous solid; $[\alpha]_D^{20}$ +57.7 (c 0.6, MeOH); UV (MeOH) λ max (log ϵ) 230 nm (3.0) and 282 nm (3.1); IR (ATR) max 3490 (br), 1620, 1502, 1450, and 935 cm^{-1}; HR-FABMS m/z 395.1294 $[M+Na]^+$ (calcd for $C_{21}H_{24}O_6Na$, 395.1305); ^1H NMR and ^{13}C NMR ($CDCl_3$) (Table 6-1).

^{1}H NMR and ^{13}C NMR (in DMSO-d_6) of compound **6**

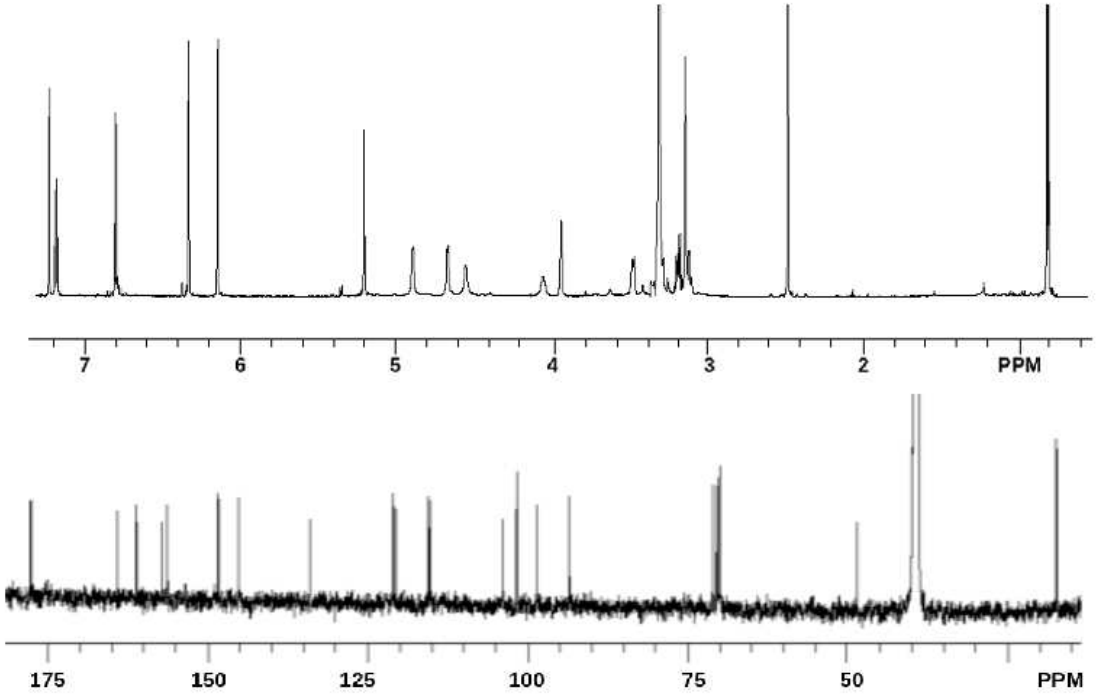

^{1}H NMR and ^{13}C NMR (in DMSO-d_6) of compound **7**

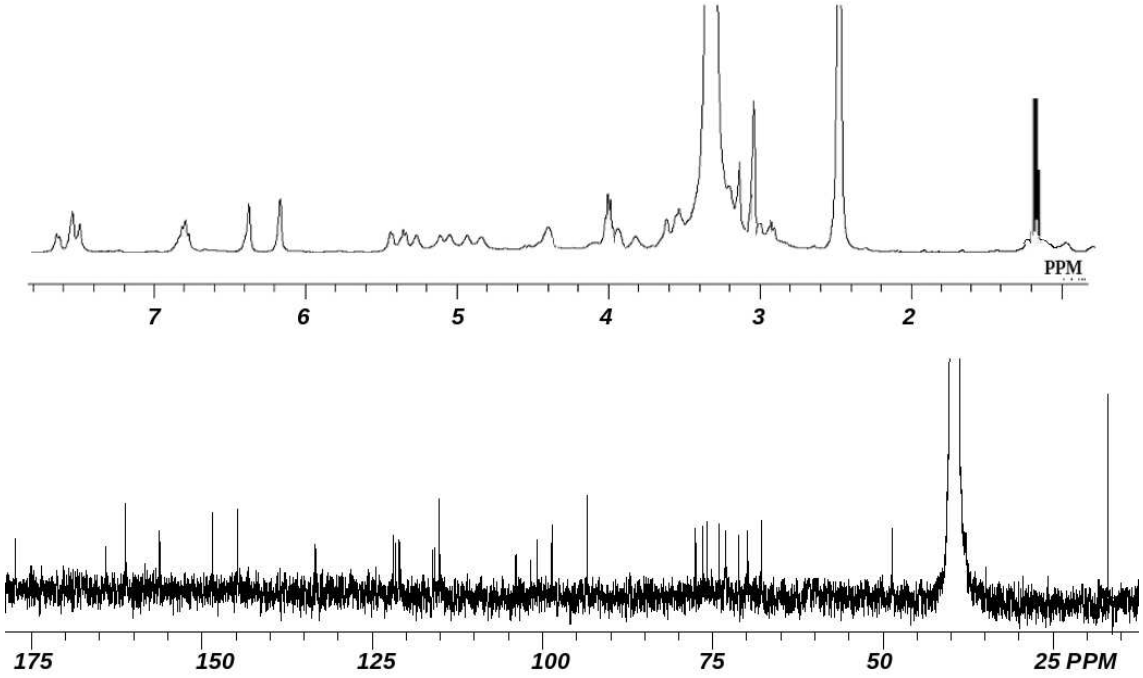

^{1}H NMR and ^{13}C NMR (in Pyridine-d_5) of compound **14**

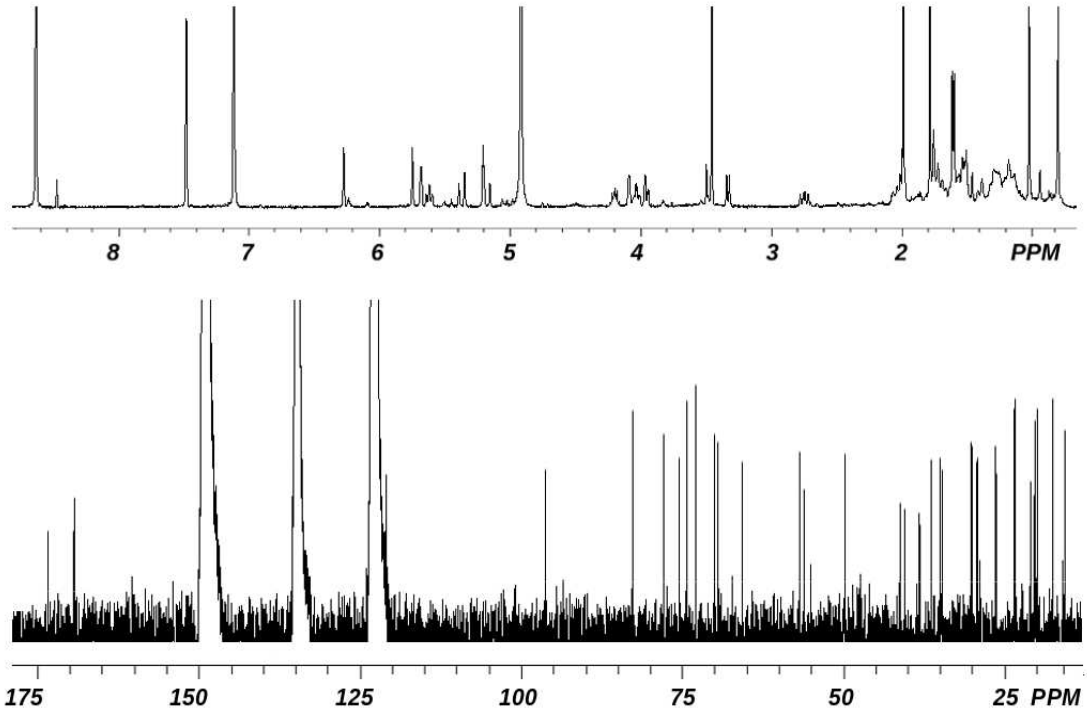

^{1}H NMR and ^{13}C NMR (in $CDCl_3$) of compound **40**

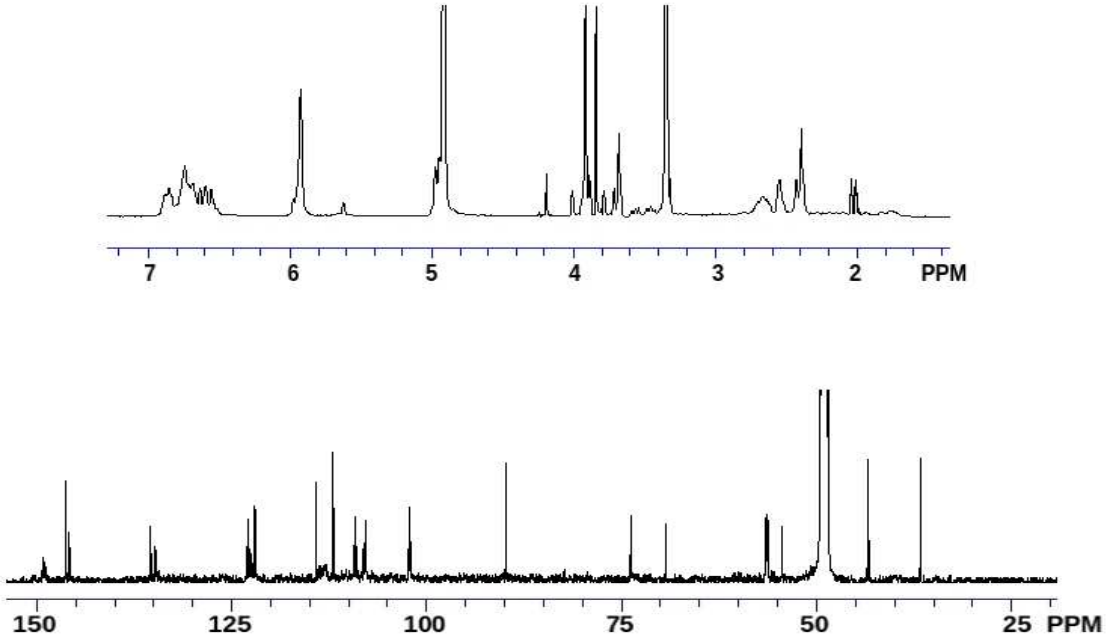

Publications

1. Rifai, Y.; Arai, M. A.; Koyano, T.; Kowithayakorn, T.; Ishibashi, M. *J. Nat. Prod.* **2010**, *73*, 995-997.

2. Rifai, Y.; Arai, M. A.; Sadhu, S. K.; Ahmed, F.; Ishibashi, M. *Bioorg. Med. Chem. Lett.* **2011**, *21*, 718-722.

3. Rifai, Y.; Arai, M. A.; Koyano, T.; Kowithayakorn, T.; Ishibashi, M. *J. Nat. Med.* **2011**, *65*, 629-632.

Honorable Referees

1. Professor Tsutomu ISHIKAWA — Chairman
   Graduate School of Pharmaceutical Sciences

2. Professor Hiromitsu TAKAYAMA — Member
   Graduate School of Pharmaceutical Sciences

3. Professor Naoto YAMAGUCHI — Member
   Graduate School of Pharmaceutical Sciences